

Review

# Recent Advances in All-Solid-State Lithium–Oxygen Batteries: Challenges, Strategies, Future

Sara Pakseresht <sup>1,\*</sup>, Mustafa Celik <sup>2,3</sup>, Aslihan Guler <sup>2</sup>, Ahmed Waleed Majeed Al-Ogaili <sup>2</sup> and Tanja Kallio <sup>1</sup>

<sup>1</sup> Department of Chemistry and Materials Science, School of Chemical Engineering, Aalto University, 02150 Espoo, Finland; tanja.kallio@aalto.fi

<sup>2</sup> Sakarya University Research, Development, and Application Center (SARGEM), Esentepe Campus, Sakarya 54050, Türkiye; mustafacelik@sakarya.edu.tr (M.C.); aslihan.guler@ogr.sakarya.edu.tr (A.G.); ahmed.waleed@uaa.edu.iq (A.W.M.A.-O.)

<sup>3</sup> Engineering Faculty, Department of Metallurgical and Materials Engineering, Esentepe Campus, Sakarya University, Sakarya 54050, Türkiye

\* Correspondence: sara.pakseresht@aalto.fi

**Abstract:** Digital platforms, electric vehicles, and renewable energy grids all rely on energy storage systems, with lithium-ion batteries (LIBs) as the predominant technology. However, the current energy density of LIBs is insufficient to meet the long-term objectives of these applications, and traditional LIBs with flammable liquid electrolytes pose safety concerns. All-solid-state lithium–oxygen batteries (ASSLOBs) are emerging as a promising next-generation energy storage technology with potential energy densities up to ten times higher than those of current LIBs. ASSLOBs utilize non-flammable solid-state electrolytes (SSEs) and offer superior safety and mechanical stability. However, ASSLOBs face challenges, including high solid-state interface resistances and unstable lithium–metal anodes. In recent years, significant progress has been proceeded in developing new materials and interfaces that improve the performance and stability of ASSLOBs. This review provides a comprehensive overview of the recent advances and challenges in the ASSLOB technology, including the design principles and strategies for developing high-performance ASSLOBs and advances in SSEs, cathodes, anodes, and interface engineering. Overall, this review highlights valuable insights into the current state of the art and future directions for ASSLOB technology.

**Keywords:** solid electrolytes; lithium–oxygen batteries; interfaces; safety



**Citation:** Pakseresht, S.; Celik, M.; Guler, A.; Al-Ogaili, A.W.M.; Kallio, T. Recent Advances in All-Solid-State Lithium–Oxygen Batteries: Challenges, Strategies, Future. *Batteries* **2023**, *9*, 380. <https://doi.org/10.3390/batteries9070380>

Academic Editor: Atsushi Nagai

Received: 15 June 2023

Revised: 8 July 2023

Accepted: 12 July 2023

Published: 17 July 2023



**Copyright:** © 2023 by the authors. Licensee MDPI, Basel, Switzerland. This article is an open access article distributed under the terms and conditions of the Creative Commons Attribution (CC BY) license (<https://creativecommons.org/licenses/by/4.0/>).

## 1. Introduction

Concern about the energy issue and environmental conservation has led to substantial investments in renewable energy technologies that are ecological, clean, and sustainable. Li-ion batteries are utilized in electric vehicles (EVs) and other energy storage technologies because of their high energy density and beneficial environmental attributes. However, the current energy density of LIBs is below  $200 \text{ Wh kg}^{-1}$ , which is insufficient to accomplish the long-term objective of EVs. Lithium–oxygen batteries (LOBs), in comparison with other battery types, such as LIBs, redox flow batteries, and lead–acid batteries, provide a significantly higher energy density. In fact, the energy density of lithium–oxygen systems can range from 3 to 30 times higher than that of commercially available LIBs. LOBs have received much attention since they were first discovered, and some breakthroughs have been made in recent decades [1]. However, major problems remain for LOBs, such as Li dendrite formation, parasite reactions, and a lack of effective electrocatalysts for the oxygen reduction reaction/oxygen evolution reaction (ORR/OER) at ambient temperature.

The all-solid-state lithium–oxygen batteries offer several advantages over the traditional liquid system of LOBs. Specifically, ASSLOBs address issues related to the volatilization of liquid electrolytes. ASSLOBs offer several significant benefits.: Firstly, they provide

improved safety compared to batteries with liquid electrolytes. Liquid electrolytes, despite their conductivity and electrode wetting capabilities, come with risks such as volatilization, leakage, and thermal failure at high temperatures. Solid electrolytes (SEs), on the other hand, exhibit high thermal stability and ionic conductivity, effectively mitigating these concerns, even at elevated temperatures. Secondly, ASSLOBs exhibit a longer life cycle and higher energy density compared with their liquid counterparts. The robust chemical and mechanical durability of SEs allows for operation at higher voltage ranges. Additionally, the elimination of side reactions between metal anodes and H<sub>2</sub>O/CO<sub>2</sub> becomes achievable, resulting in an extended lifespan for the battery.

ASSLOBs are still in their infancy, and there are numerous barriers preventing their widespread implementation. The lifetime of batteries can be greatly affected by side reactions and the formation of dendrites, which are attributed to the inherent electrodeposition properties and reactivity of lithium metal anodes. Additionally, the large volume variation of lithium during cycling results in an unstable interface, ultimately compromising the battery's cycle span. The severe volume variation of lithium is attributed primarily to three factors: the intrinsic hostless nature of Li deposition, the growth of Li dendrites, and the accumulation of inactive Li debris. The plating and stripping of Li exhibit a hostless behavior, leading to the uncontrolled expansion and contraction of Li volume during repetitive charge and discharge cycles. Second, solid electrolytes frequently display a substantial interface resistance because of poor contact with the electrode. Lastly, the multistep reaction mechanism of a solid-state system remains unknown, and how to develop an effective catalyst requires further investigations.

One of the key advantages of ASSLOBs is their potential for increased safety. Solid-state electrolytes eliminate the risks associated with volatile and flammable liquid electrolytes, making ASSLOBs less prone to leakage, thermal runaway, and fire hazards. This makes them attractive for applications where safety is paramount, such as EVs and portable electronics. In terms of energy density, ASSLOBs have the potential to achieve much higher energy densities compared with traditional LIBs. This is due to the high theoretical energy density of lithium–oxygen chemistry. ASSLOBs could enable EVs to achieve longer driving ranges and portable electronic devices to have extended usage times.

Moreover, ASSLOBs offer improved cycle life compared with conventional LIBs. The use of solid-state electrolytes helps mitigate electrode degradation, dendrite formation, and side reactions, leading to longer-lasting batteries. This translates to reduced maintenance and replacement costs, making ASSLOBs economically advantageous. The potential applications for ASSLOBs are wide-ranging. Electric vehicles stand out as a major application area. ASSLOBs could offer EVs longer driving ranges, faster charging times, and increased safety, addressing some of the limitations of current LIBs. Additionally, ASSLOBs can find applications in grid-scale energy storage, where their high energy density and improved cycle life can contribute to more efficient and reliable energy storage systems.

The increasing adoption of EVs and the growing need for grid-scale energy storage are driving the demand for advanced battery technologies. ASSLOBs have the potential to address the limitations of existing energy storage systems, offering higher performance, improved safety, and longer lifespans. However, further research and development efforts are required to overcome the technical challenges and optimize the performance and scalability of ASSLOBs before they can reach widespread commercialization.

Here, we will highlight the core progress and critical issues of ASSLOBs and concentrate on some issues and challenges faced by various types of SEs. This review will be a beneficial resource for the progress of ASSLOBs and will shed light on the areas where researchers should focus their future research efforts. Nevertheless, research in this field continues to make substantial advances, and it is predicted that ASSLOBs will serve as a key factor in the development of sustainable energy storage solutions. Additionally, digitalization and machine learning (ML) efforts in SE materials and recycling and alternative recovery methods for ASSLOBs are discussed. Digitalization and ML efforts in SE materials can revolutionize the development of advanced energy storage technologies by

accelerating material discovery, optimizing material properties, and guiding experimental efforts toward more efficient and sustainable battery technologies. In addition, recycling can help recover valuable materials from spent batteries, minimizing reliance on primary resources. Research is being conducted on innovative extraction and recovery methods to reduce the environmental impact and increase the efficiency of obtaining materials.

In summary, ASSLOBs have the potential to revolutionize energy storage and provide a safe, high-density alternative to traditional batteries. However, much work still needs to be done to overcome the technical challenges that are currently hindering their widespread adoption. This article provides a comprehensive overview of the present status within the field and highlights some of the most urgent concerns that must be tackled to unlock the complete potential of ASSLOBs.

### 1.1. The Principal Operation of Lithium–Oxygen Batteries

Since Abraham and Jiang introduced them in 1996, lithium–oxygen systems have been projected as a widespread energy storage application due to their high theoretical energy density ( $3500 \text{ Wh kg}^{-1}$  based on mass of oxygen). However, LOB systems evolved relatively slowly over the next few decades due to their poor rate capability and limited life cycle. In 2006, Bruce and his colleagues represented the reversible dissolution of  $\text{Li}_2\text{O}_2$  in the LOB system, resulting in a renewed surge of interest in the LOB system [2]. A lithium–oxygen system typically consists of a lithium metal as the anode, oxygen serving as the active cathode material, and an electrolyte solvent containing  $\text{Li}^+$  salt (Figure 1). Regarding the electrolyte, the LOB system can be categorized into four types: aqueous, non-aqueous, hybrid, and solid-state. The electrode reaction mechanism in a non-aqueous LOB system ( $\text{Li} + \text{O}_2 \rightarrow \text{Li}_2\text{O}_2$  2.96 V versus  $\text{Li}/\text{Li}^+$ ) differs from that in an aqueous LOB system ( $4\text{Li} + 2\text{H}_2\text{O} + \text{O}^{2-} \rightarrow 4\text{LiOH}$  3.4 V vs.  $\text{Li}/\text{Li}^+$ ). However, conventional LOBs that are based on liquid electrolytes show significant safety issues. These issues arise due to the leakage of organic liquid electrolytes and the uneven deposition of  $\text{Li}^+$  on the lithium metal negative electrode [3].

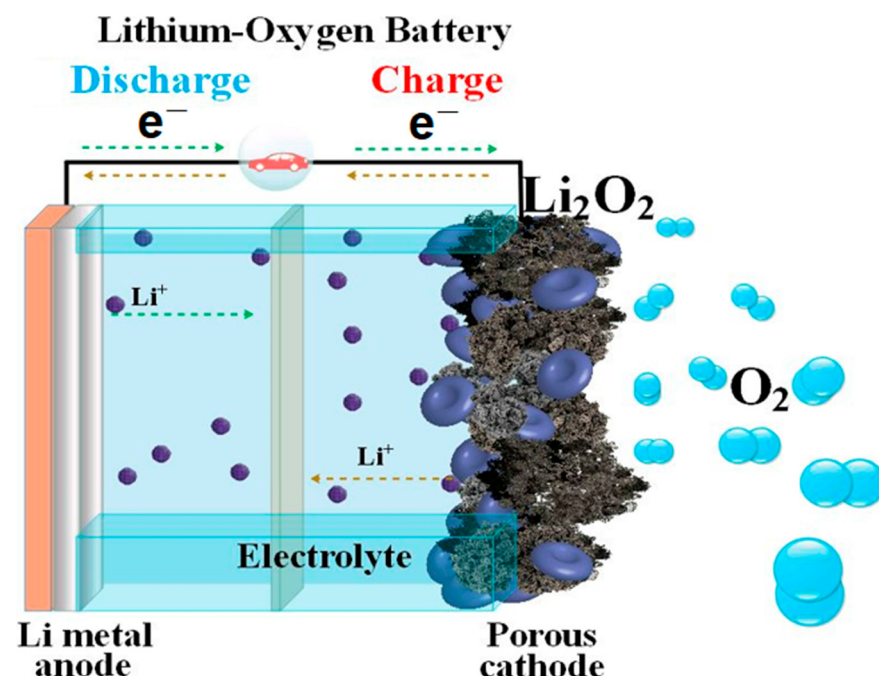


**Figure 1.** The schematic illustrates the basic concept of lithium–oxygen batteries. A porous air cathode, Li metal anode, and an electrolyte are the three main components of any such system.

## 1.2. Challenges in Lithium–Oxygen Batteries

In lithium–oxygen systems, electrolytes are essential for dissolving oxygen and transporting  $\text{Li}^+$  between the cathode and anode. In addition, a good-performing electrolyte with high chemical and electrochemical durability, minimal evaporation, good ionic conductivity, low viscosity, significant oxygen solubility, and diffusion coefficient can enhance the LOB performance. One of the main obstacles to widespread use of LOBs is the instability of the electrolyte. Here, further challenges in LOB electrolytes are discussed.

**Electrolyte stability and ionic conductivity.** One essential prerequisite for intrinsically safe solid-state LOBs is the implementation of appropriate SSEs. Solid-state electrolytes are selected over liquid electrolytes owing to their enhanced safety and stability, but they are still prone to chemical reactions with the lithium anode or the oxygen cathode, resulting in poor battery performance and reduced cycle life [3,4]. To overcome this challenge, researchers have developed new solid-state electrolytes with improved stability, such as sulfide-based electrolytes and garnet-type electrolytes [5,6]. The electrolyte in the LOB system is responsible for the transport of  $\text{Li}^+$  ions between the anode and cathode, as well as the oxidation and reduction reactions that occur upon charge and discharge [7,8]. Therefore, the appropriate selection of the electrolyte is crucial to the performance and durability of the battery [9]. One major challenge in developing electrolytes for SSLOBs is achieving high ionic conductivity at room temperature. Solid-state electrolytes typically have lower conductivity than liquid electrolytes, and this can limit the rate capability and power density of the batteries [10]. Another challenge is the compatibility of the electrolyte with the cathode material [11,12]. The cathode used in LOBs typically consists of a porous carbon material, and it is crucial for the electrolyte to effectively permeate the pores and interact with the cathode material without triggering undesired side reactions or deterioration. This ensures optimal performance and durability of the battery system. Furthermore, the stability of the electrolyte during cycling is essential to the long-term performance and safety of the battery. Electrolyte degradation can lead to the generation of unwanted reaction products and the accumulation of solid-state deposits that can block ion transport and reduce the battery capacity [13]. To address these challenges, many research studies have investigated various classified electrolytes, including polymer electrolytes (PEs), ceramic electrolytes, and composite electrolytes (CEs). Overall, the progression of high-performance electrolytes for ASSLOBs is a critical research area that will enable the practical application of this promising energy storage technology.

**Electrode–Electrolyte Interface.** The other major challenge in the advancement of ASSLOBs is the electrode–electrolyte interface. The formation of a stable and low-resistance interface between the solid-state electrolyte and the Li anode or the oxygen cathode is pivotal for the efficient operation of the battery. However, the interface can be impacted by different factors, including the roughness of the electrode surface, the composition of the electrolyte, and the presence of impurities [14]. To address this challenge, researchers have explored various surface modification techniques, such as a protective layer for the electrode surface or the introduction of additives to the electrolyte [15,16].

The stable solid electrolyte interface (SEI) layer formation at the electrode–electrolyte interface is vital for the performance and durability of ASSLOBs [17], although the formation and evolution of the SEI layer is a complex process that is influenced by various parameters, including the composition of the electrolyte and the electrode surface structure. Recent studies have proposed different strategies to control the SEI layer formation, including the use of additives in the electrolyte and the modification of the electrode surface [18–21]. For instance, a recent work by Paul et al. [22] reported that the addition of a small amount of vinylene carbonate to the electrolyte could improve the SEI layer formation and boost the cycling performance of the battery.

The ORR kinetics at the electrode–electrolyte interface is another major factor that affects the performance of SSLOBs [23,24]. To improve the ORR kinetics, various catalysts have been proposed, such as noble metals (e.g., Pt and Pd) as well as non-noble metals (e.g., Fe and Co) [25,26]. For example, an investigation by Liu et al. [27] found that the

use of a Co-based catalyst could promote both the ORR kinetics and the overall cycling performance of the battery.

The high reactivity between lithium and the electrolyte can result in the formation of an unstable interface, which poses a significant risk of battery failure [28]. The ASSLOB systems are also susceptible to lithium dendrite growth, which can lead to short circuits and battery fading. To address this challenge, various strategies have been proposed, including using solid electrolytes with high Li ion conductivity and the modification of the electrode surface to reduce the local electric field [29–32]. Guangmei et al. [33] showed that a  $\text{Li}_{1.5}\text{Al}_{0.5}\text{Ge}_{1.5}(\text{PO}_4)_3$  solid electrolyte could suppress lithium dendrite formation and enhance the battery performance.

**Low Operating Temperature.** SSLOBs are a promising energy storage technology, but they face several challenges related to low operating temperatures. At low temperatures, the mobility of Li ions and the kinetics of oxygen reduction reactions decrease, which can lead to poor battery performance [34]. To overcome these challenges, researchers have investigated various approaches to achieve low-temperature operation, such as using SSEs with high ionic conductivity, developing new cathode materials with high activity at low temperatures, and optimizing the battery design [35–38]. For example, the  $\text{RuO}_2$ -based air cathodes can enhance the low-temperature performance of ASSLOBs by improving the oxygen reduction reaction kinetics [39]. Furthermore, recent studies have investigated the utilization of SSEs such as  $\text{Li}_7\text{La}_3\text{Zr}_2\text{O}_{12}$  (LLZO) and  $\text{Li}_{1.575}\text{Al}_{0.5}\text{Ge}_{1.5}(\text{PO}_4)_3$  (LAGP) to overcome the low-temperature challenges [40]. While the low-temperature challenges for SSLOBs batteries are significant, researchers are making progress in developing new strategies to overcome these challenges and enhance the stability of these batteries at low temperatures.

**Mechanical Properties.** The mechanical properties of ASSLOBs, such as their flexibility, toughness, and fracture resistance, are also important for their practical application. The ASSLOB systems typically use solid-state electrolytes, which offer several benefits over liquid electrolytes, including increased safety, stability, and energy density. However, inorganic solid-state electrolytes are often brittle and have poor mechanical properties, which can lead to cracking or delamination of the electrode–electrolyte interface and ultimately reduce the battery’s performance and lifetime. Therefore, improving the mechanical properties of SSEs is critical for the advancement of high-performance ASSLOBs [41–43].

One strategy for enhancing the mechanical features of SSEs is through the incorporation of various fillers, such as polymers, ceramic particles, and carbon materials, into the electrolyte matrix. These fillers can improve the elasticity, toughness, and adhesion of the electrolyte, thereby reducing the risk of cracking or delamination at the electrode–electrolyte interface. For instance, researchers have reported the use of polymers, such as polyethylene oxide (PEO) [44], polyvinylidene fluoride (PVDF) [45], and poly(methyl methacrylate) (PMMA) [46], as fillers in SSEs, which can significantly enhance the mechanical features of the electrolyte and improve the battery’s cycling stability and rate capability [47].

In addition to filler incorporation, the use of advanced processing techniques, such as freeze-casting, electrospinning, and 3D printing, can also improve the mechanical properties of solid-state electrolytes. For example, freeze-casting can create highly aligned and porous electrolyte structures, which can improve the electrolyte’s mechanical strength and ion transport properties [48]. Electrospinning can produce nanofibrous electrolyte membranes with high surface area and mechanical strength, while 3D printing can create complex and customized SSE structures with improved mechanical properties and interfacial compatibility [49–51]. Overall, improving the mechanical properties of SSEs is a crucial challenge in the development of high-performance ASSLOBs. Addressing this challenge requires a multidisciplinary approach that involves materials science, chemistry, and engineering, and the use of cutting-edge processing techniques and fillers.

**High Process Costs.** The ASSLOBs have been the subject of research for their potential to provide high energy density and safety. Nevertheless, the development of these batteries

continues to encounter various challenges, with one notable obstacle being the high costs associated with the manufacturing processes involved. One of the main reasons for the high process costs of ASSLOBs is the need for specialized materials and manufacturing processes. Solid-state electrolytes and electrode materials with ideal properties for LOBs are still in the development phase, and their synthesis can be expensive. Additionally, the fabrication process of ASSLOBs is more complicated compared with conventional Li-ion batteries, which adds to the overall process costs. Several approaches have been proposed to solve the high process costs of solid-state lithium batteries [52,53]. One approach is to develop cost-effective manufacturing methods that use inexpensive precursors and equipment. For instance, in some studies, researchers developed a method for preparing an SSE using a simple sol–gel process, which reduced the overall cost of the electrolyte [54,55]. Another approach is to develop materials that can be synthesized at a lower cost [56,57]. Furthermore, studies have also explored the use of scalable manufacturing techniques, such as roll-to-roll processing, to lower the manufacturing costs of SSLOBs. Roll-to-roll processing involves the continuous deposition of materials onto a flexible substrate, which can reduce the overall cost of the battery production process [58]. Overall, addressing the high process costs of SSLOBs requires the development of cost-effective materials and production processes, as well as the adoption of scalable and efficient production methods.

Finally, the commercial viability of ASSLOBs has yet to be proven. It is a huge challenge for low-efficiency ASSLOBs. Oxygen consumption and high energy savings can cause batteries to have low efficiency. To meet these needs, it is necessary to optimize the layers and electrode materials and to optimize the operating conditions of the batteries, such as temperature and pressure. These batteries are still prototype tests and further research and development is required for commercial production and marketing. In addition, production costs and production methods should be optimized. Structures built on ASSLOBs demonstrate the importance of these batteries, but their use also has many challenges. More research and development work are required to create clusters of these sections.

## 2. All-Solid-State Lithium–Oxygen Batteries

In particular, ASSLOBs have garnered significant attention in recent years. One major advantage of these batteries is their capability to prevent solvent evaporation and inhibit undesirable parasite reactions between reactive metal anodes and contaminant gases (such as  $\text{H}_2\text{O}$  and  $\text{CO}_2$ ). However, there are still many difficulties with ASSLOBs, including Li dendrite formation, high interface resistance, and the absence of an effective catalyst. In addition, LOBs require extremely stable electrolytes due to the attack of activated oxygen in unstable electrolytes, causing them to degrade quickly. In the following sections, further discussion of the aforementioned issues is given.

### 2.1. Lithium Metal Anode for Solid-State Lithium–Oxygen Batteries

Li metal is an excellent anode material owing to its high theoretical energy density ( $3860 \text{ mAh g}^{-1}$ ) and low potential (0.304 V vs. standard hydrogen electrode (SHE)). However, in conventional LOBs, significant issues arise, including safety hazards associated with organic electrolytes, the formation of harmful SEIs, electrolyte decomposition and evaporation, and the formation of dendrites due to the Li metal anode corrosion [41]. Dendrites formed and volumetric changes on the Li anode during Li coating/stripping cause a low cycle number [59]. The morphology and components of SEI formed at the electrolyte/Li interface are affected by the reaction of the Li anode with  $\text{H}_2\text{O}$ ,  $\text{O}_2$ , and intermediates ( $\text{LiOH}$ ,  $\text{Li}_2\text{O}$ ,  $\text{Li}_2\text{CO}_3$ , etc.) during the electrochemical process [60]. Another difficulty with LOBs is the instability of the electrolyte due to the decomposition at high voltage and forming parasite products [61]. Additionally, a small amount of liquid electrolyte is generally used to decrease the interface resistance between the Li metal anode and the electrolyte, and the continuous consumption of liquid electrolytes during the cycle cannot be prevented [38]. In order to inhibit the contact of  $\text{H}_2\text{O}$  and  $\text{O}_2$  at the Li metal anode, some

methods such as coating the Li surface with an artificial protection film, modifying the electrolyte/sePARATOR, and alloying the anode have been studied in the literature [62].

Recent studies proceed to investigate the physical and chemical stability of the contact between the Li metal anode and SE. In earlier reports, a slight amount of liquid electrolyte is typically injected to minimize the interface resistance between the Li metal anode and the electrolyte. Yet, the constant use of liquid electrolytes during cycling is not entirely feasible. It is hypothesized that even at higher current densities, the surface coating with lithophilic compounds can effectively inhibit the Li penetration. The application of a coating material, such as metals, metal oxides, or sulfides, can facilitate the formation of a uniform interface by reacting with the metal anode. This results in the creation of a high Li-ion transport pathway, which facilitates an efficient charge transfer while preventing undesirable side reactions. Another prominent method for inhibiting the formation of Li dendrites is polymer interlayers. The SEI layer is mechanically unsteady because of the massive ion flow at the interface and the massive volume variation in the Li anode. Lithium alloys prevent dendritic formations in LOBs, effectively reducing the excessive nucleation potential of Li and lowering the interfacial resistance [63]. Deng et al. [64] obtained a  $\text{Li}_{21}\text{Si}_5$  alloy by alloying the Li anode with Si and obtained a capacity of approximately 1000  $\text{mAh g}^{-1}$  after approximately 80 cycles. While these alternative alloy anodes reduce certain issues associated with the Li metal, they generally have a limited Li source. The use of a heavier element apart from Li in the anode part will cause a decrease in the energy density of the LOBs after a while [65]. On the other hand, the three-dimensional (3D) freestanding anodes prevent volume expansion in the Li metal, thanks to their large surface areas and the voids [66]. Thus, a composite Li metal that exhibits improved cycling stability and dendrite-free characteristics is formed for LOBs. To illustrate the role of the lithium anode in the formation and decomposition of  $\text{Li}_2\text{O}_2$  at the cathode, Jeong et al. [67] designed a 3D host–lithium composite anode for LOBs using Cu. In comparison with LOBs made of Li metal, this composite anode demonstrated lower polarization, improved rate capability, and cycle stability. Ma et al. [68] produced a graphene aerogel/Li freestanding anode by utilizing the porous and conductive skeleton of graphene aerogel and obtained improved cycling stability over 700 cycles. However, while 3D anodes reduce the energy density for LOBs, the high surface area elevated the possibility of side reactions [61]. Luo et al. [69] provided stable SEI formation on the surface of anode by coating the Li metal anode surface with  $\text{SiO}_2/\text{GO}$ . As a result, they obtained a capacity of approximately 1000  $\text{mAh g}^{-1}$  after approximately 300 cycles, preventing chemical corrosion of the anode. As a different approach, *in situ* passivation or SEI film formation on the Li metal anode is seen as one of the potential methods to solve the problem of dendrite formation and volume change on the Li anode. Furthermore, the use of inorganic materials that interact with Li-metal anodes while forming alloys effectively decreases the interface resistance [70].

In conclusion, improving the anode–electrolyte interface in ASSLOBs is crucial for enhancing their electrochemical performance. Following are some perspectives to improve this issue:

**Developing advanced interfacial materials.** Advanced interfacial materials, such as solid-state electrolytes and interlayers, can enhance the contact of the anode with electrolyte by preventing the formation of harmful SEIs, reducing polarization, and promoting ion transport.

**Surface modification of the anode.** Surface modification techniques, such as surface coating, can improve the wettability of the anode and enhance the contact between the anode and the electrolyte. For example, the use of hydrophilic coatings can promote the adsorption of electrolyte species and enhance their diffusion.

**Designing porous anodes.** Porous anodes with high surface area can enhance the contact of the anode with the electrolyte, facilitating the diffusion of ions and oxygen. This can be achieved by utilizing materials with high porosity, including carbon-based materials or metal oxides, and by controlling the morphology of the anode.

Using 3D printing technology. Three-dimensional printing technology can be used to fabricate anodes with precise geometry and control the distribution of pores and active materials, which can provide a good contact of the anode with the electrolyte.

Conducting *in situ* characterization. *In situ* characterization techniques, such as electrochemical impedance spectroscopy and scanning electron microscopy, can be employed to monitor the anode–electrolyte interface and identify the factors that affect their contact. This information can be used to optimize the design and composition of the anode and electrolyte to improve their contact.

Recently, researchers have proposed anodeless Li batteries to increase the energy densities of Li batteries [71]. In lithium-free batteries, Li ions from the cathode during the charging process form a thin Li film on the negative current collector. This unique lithium battery design can deliver ultra-high energy density of approximately 400 Wh/kg or 1200 Wh/L [72]. Anodeless Li batteries are seen as a solution to the abnormal heating, explosion, and combustion problem caused by liquid electrolytes, as well as the formation of dendrites and unstable SEI. In anodeless Li batteries in which organic liquid electrolyte is used, carbonate-weighted SEI is formed, which causes a capacity loss because of the decomposition of the organic electrolyte. In recent years, there have been reports on the integration of an anodeless configuration within all-solid-state battery systems as a means to enhance safety. By utilizing non-flammable SEs, the issue of thermal runaway can be significantly reduced compared with batteries employing flammable organic liquid electrolytes. Additionally, the robust mechanical strength of the SE serves to mitigate the Li dendrite growth towards the cathode, thereby minimizing the potential for short-circuiting. Nikodimos et al. [73] produced an anodeless solid state Li battery by filling PVDF-HFP gel electrolyte with LAMGP ( $\text{Li}_{1.6}\text{Al}_{0.5}\text{Mg}_{0.1}\text{Ge}_{1.5}(\text{PO}_4)_3$ ) filler. The anodeless cell prepared with a polymer matrix composite electrolyte showed high mechanical strength, high ionic conductivity, and electrochemical stability at room temperature. Electrostatic interaction between the gel polymer membrane and the current collector formed a good adhesion. In the anodeless Li battery, a safe interface chemistry was created, and the dendrite growth was suppressed thanks to the composite gel polymer electrolyte.

## 2.2. Solid Electrolyte for Lithium–Oxygen Batteries

Many efforts have been made to discover an optimal electrolyte configuration. Solid electrolytes emerge as one of the most explored strategies for enhancing the safety of rechargeable lithium batteries, as they inhibit leakage, volatilization, and ignition. Typically, ceramics and polymers are utilized as SEs in solid-state battery (SSBs) systems.

The solid electrolyte is considered as the fundamental element of the SSBs. The main function of SEs is to separate the anode and cathode from each other and create a transition zone for the transportation of Li ions. The function of the SEs necessitates meeting certain requirements. First, the ionic conductivity of the SE at room temperature should be more than  $10^{-4}$  S cm<sup>-1</sup>. At the same time, the electronic conductivity of the SE is expected to be negligible, and its electrochemical stability is expected to be high. Solid electrolytes could be broadly categorized into two major groups: inorganic electrolytes and organic electrolytes. The different properties of inorganic and organic electrolytes are compared in Figure 2a.

**Inorganic electrolytes:** NASICON-, garnet-, perovskite-, LISICON-, LIPON-, and sulfur-based electrolytes are notable examples of inorganic electrolytes that fulfill these requirements. The advantages and challenges of these inorganic SSEs are presented in Table 1, and radar plots of some properties of these inorganic SSEs are given in Figure 2b. Inorganic sulfide-based solid electrolytes, among the mentioned options, are not suitable for SSLOBs due to concerns related to their high sensitivity to humidity, which can lead to the risky leakage of toxic H<sub>2</sub>S. In the context of SSLOBs, it is preferable to use inorganic oxides and solid electrolytes such as NASICON, garnet, perovskite, anti-perovskite, and zeolite, as they offer more favorable characteristics for the operating environment (Figure 2c).

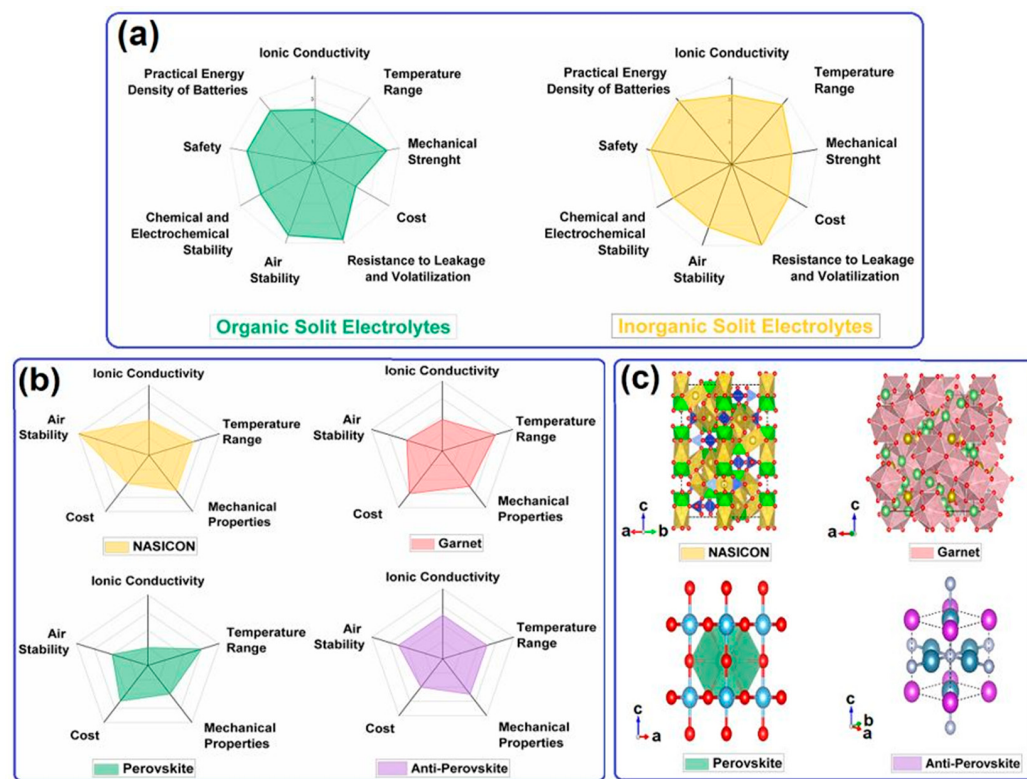


**Figure 2.** (a) Inorganic and organic electrolytes are compared in terms of cost, safety, and chemical and mechanical properties. (b) Performance of various SSE materials is assessed and compared by radar plots, which illustrate properties of different SSEs. (c) The NASICON-type, perovskite-type, garnet-type, and zeolite-type SSEs crystal structures.

**Table 1.** Properties of inorganic SSEs.

SSEs	Typ.	Advantages	Challenges	$\sigma_{\text{Li}}$ ( $\text{S cm}^{-1}$ )	Refs.
Oxide-based	NASICON and LISICON	Air stability and mechanical strength Substitution, composite material, and protective layer	Li anode instability	$10^{-5}\text{--}10^{-3}$	[74–78]
	Garnet	Stability with Li metal and mechanical strength Substitution, protective layer, changing the ratio of $\text{Li}^+$ , and introducing additives	Sensitive to $\text{CO}_2$ and humidity	$10^{-5}\text{--}10^{-3}$	[79–83]
	Perovskite	Air stability, low cost, and mechanical strength Substitution and composite material	Li anode instability	$10^{-5}\text{--}10^{-3}$	[84–88]
Sulfide-based	Thio-LISICON and $\text{Li}_2\text{S}-\text{M}_x\text{S}_y$	High $\sigma_{\text{Li}}$ Substitution, composite material, and ion exchange	Sensitive to $\text{O}_2$ and humidity	$10^{-4}\text{--}10^{-2}$	[89–93]
Other type	Anti-perovskite	Stability with Li metal and light weight substitution	Poor cycling and structural durabilities	$10^{-4}\text{--}10^{-2}$	[94–97]
	LiPON	Li metal stability and mechanical rigidity Properties of bond and functional group	Low $\sigma_{\text{Li}}$ and expensive	$10^{-6}$	[98,99]

NASICON (sodium superionic conductor) is a family of SSEs with the general formula  $\text{Na}_{1+x}\text{Zr}_2\text{Si}_x\text{P}_{3-x}\text{O}_{12}$  (where  $x$  is typically between 0.5 and 2) and has been investigated

for use in various energy storage devices [100]. Typically, these materials adopt the formula  $AM_2(PO_4)_3$ , with the A site accommodating elements such as Li, Na, or K, while the M region is commonly occupied by Ge, Zr, or Ti. In particular, the  $Li_{1+x}M_xTi_{2-x}(PO_4)_3$  ( $M = Al, Cr, Ga, Fe, Sc, In, Lu, Y, or La$ ) system has been extensively investigated [7,101]. LATP ceramic, which is commonly used in SSLOBs, has high ionic conductivity at ambient temperatures above  $10^{-4}$  S cm $^{-1}$ . Similarly,  $Li_{1.5}Al_{0.5}Ge_{1.5}(PO_4)_3$  has been extensively investigated due to its high ionicity ( $2.4 \times 10^{-4}$  S cm $^{-1}$ ) and relatively broad electrochemical durability window. However, when LATP or LAGP comes into contact with a Li anode, the presence of  $Al^{3+}$  and  $Ge^{4+}$  in the electrolyte tends to undergo reduction by the Li metal, resulting in the formation of a Li-Al alloy or Li-Ge alloy. This limits the use of these SEs with a Li metal anode. Various strategies such as ion exchange or coating the surface with polymer electrolyte have been developed to stabilize the electrolyte/Li anode interface in recent studies [102,103]. Recent research has shown promising results for NASICON-type solid electrolytes in ASSLOBs, with improvements in cycling stability, capacity retention, and rate capability. However, issues still remain in optimizing the properties of the NASICON-type solid electrolytes for practical application, such as reducing the interfacial resistance, improving the mechanical strength, and enhancing the compatibility with cathode materials. NASICON-type SEs exhibit significant potential for implementation in ASSLOBs, and current research endeavors are dedicated to tackling the remaining obstacles while advancing the progression of robust and high performing solid-state energy storage systems.

The garnet structure is defined by a space group described by the general formula  $A_3B_2(XO_4)_3$ , where A can represent elements such as Ca, Mg, Y, or La, and B can represent elements such as Al, Fe, Ge, or Mn. The garnet material stands out as a highly promising solid-state electrolyte due to its exceptional attributes, including a broad temperature range and broad electrochemical window. When the X sites are occupied by Li atoms, the garnet-type  $Li^+$  conductor can form as  $Li_3A_2B_2O_{12}$  [104,105]. Murugan et al. [106] investigated a plate-like Li7-type garnet, namely  $Li_7La_3Zr_2O_{12}$  (LLZO,  $7.74 \times 10^{-4}$  S cm $^{-1}$ ). With subsequent studies, such as  $Li_{6.4}La_3Zr_{1.4}Ta_{0.6}O_{12}$  ( $1.0 \times 10^{-3}$  S cm $^{-1}$ ) [101] and  $Li_{6.55}Ga_{0.15}La_3Zr_{2.5}O_{12}$  ( $2.06 \times 10^{-3}$  S cm $^{-1}$ ) [107], Li ion conductivity reached high levels. Despite reaching an acceptable ionic conductivity, garnet-type SEs increase sensitivity to moisture and CO<sub>2</sub> and increase the unexpected Li dendrite formation due to irregular interfacial contact [108]. A metal-doping strategy was attempted to improve the air stability of garnet-type SEs. According to Kobi et al. [109], the co-doping of Al and Mg in lithium lanthanum zirconate ( $Li_7La_3Zr_2O_{12}$ : LLZO) demonstrated enhanced air stability. Recent investigations have revealed the effectiveness of elemental doping (e.g., Ga, Nb, Ta, and La) in garnet-type solid electrolytes for improving air stability [82,110–112]. Furthermore, the application of a protective coating was shown to be a viable approach to enhance air stability [113,114].

SSEs with a perovskite structure typically follow a general formula of  $ABX_3$ , where A represents a rare earth or alkaline earth metal, B represents a transition metal, and X denotes an anion, commonly oxygen. The crystal structure of perovskites allows the incorporation of a wide variety of cations and anions, leading to tunable properties including ionic conductivity and stability. Perovskite-type SSEs are seen as promising candidates for SSBs with their tunable properties. As an example,  $Li_{3/8}Sr_{7/16}Ta_{3/4}Zr_{1/4}O_3$  (LSTZ,  $2.7 \times 10^{-4}$  S cm $^{-1}$ ),  $Li_{3x}La_{2/3-x}TiO_3$  (LLTO,  $3.7\text{--}1.4 \times 10^{-5}$  S cm $^{-1}$ ), and perovskite-type SSEs have been reported acceptable ionic conductivity values of  $10^{-4}$  S cm $^{-1}$  [84,115]. The LLTO solid electrolyte has had applications in solid state LABs but has been reported to have unstable interfaces with the lithium anode, which limits these applications. Doping the LLTO solid electrolyte is quite difficult due to the extremely small width of the unit cell. The LSTZ solid electrolyte suffers from air stability problems. Goodenough et al. have shown that ion exchange and polymer mixing are effective in solving this issue [87,116]. Goodenough et al. [116] reported that by combining the LSTZ SE with the PEO polymer electrolyte, they successfully resolved the issue of the LSTZ SE's contact with the lithium anode. Simultaneously, this combination enhanced the stability of the polymer electrolyte.

Figure 3a,c illustrate that the perovskite LSTZ SE displays a complete blackening when in contact with a Li metal (Figure 3a). On the other hand, there is no observable change in the PEO/LSTZ combination. In Figure 3b, the XRD curves are presented after the pure and Li metal anode, which proves the reduction of the LSTZ SE. Figure 3d–e depict the voltage–time profiles measured in symmetric cells, specifically the  $\text{Li} \mid \text{PEO}/\text{LiTFSI} \mid \text{Li}$  and  $\text{Li} \mid \text{PEO}/\text{LSTZ} \mid \text{Li}$  configurations. The experimental results revealed that the PEO/LSTZ solid electrolyte demonstrated excellent performance, remaining stable for more than 700 h. However, the symmetric cell with PEO/LiTFSI was disrupted after 200 h. This result indicates that the LSTZ filler effectively inhibits the growth of the Li dendrite.

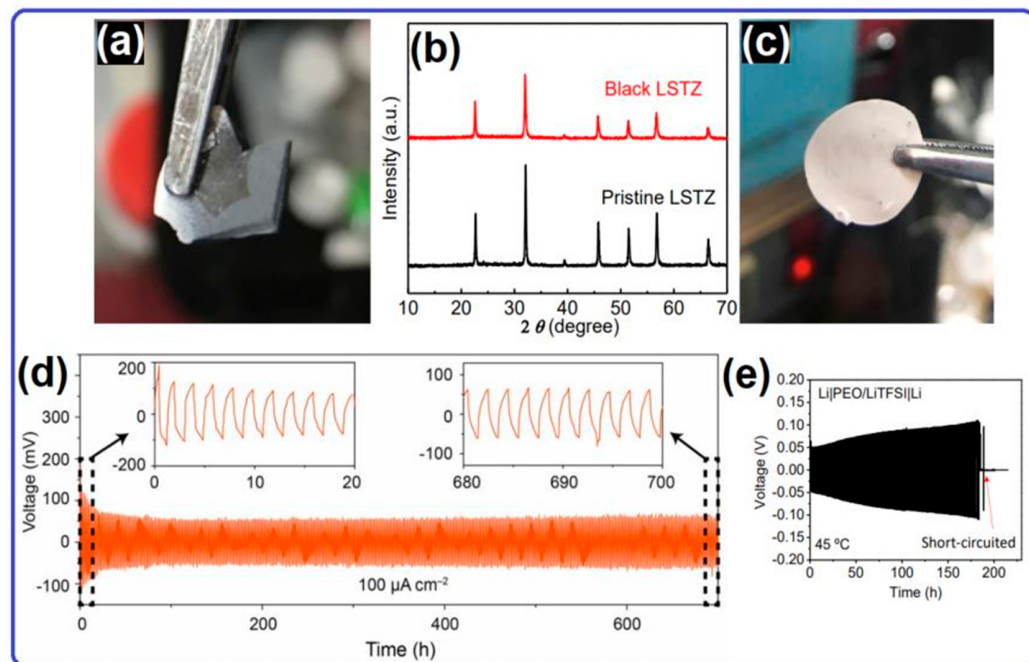


**Figure 3.** (a) LSTZ pellet after contacting the Li metal. (b) Comparative XRD patterns of pristine LSTZ and black LSTZ pellets. (c) PEO/LSTZ membrane retrieved from cycled symmetric lithium cell. Voltage–time profile of  $\text{Li} \mid \mid \text{Li}$  symmetric cell cycled at  $100 \mu\text{A cm}^{-2}$  and  $45^\circ\text{C}$ . (d) PEO/LSTZ. (e) PEO/LiTFSI. Reproduced with permission from Ref. [116]. Copyright 2019, National Academy of Sciences.

The anti-perovskite-type SE is a distinct class of solid electrolyte material characterized by its unique crystal structure, which is the inverse of the perovskite structure. In this structure, the anion sublattice of a perovskite is replaced by a cation sublattice, and the cation sublattice is replaced by an anion sublattice. This results in the formation of a new crystal structure with different properties. These electrolytes have a chemical formula of  $\text{Li}_3\text{OA}$ ,  $\text{Li}_{(3-x)}\text{M}_{x/2}\text{OA}$ , where A is an anion and M is a metal cation [117]. Anti-perovskites ( $\text{Li}_2\text{OHX}$ , where X = Cl, Br, F) are a specific type of anti-perovskite solid electrolyte that have high ionic conductivities, low-temperature processability, and a high electrochemical stability window [118]. Recent studies have shown that Li-rich anti-perovskite  $\text{Li}_2\text{OHBr}$ -based PEs can be utilized as a flexible SSE to promote the performance of batteries [119]. Anti-perovskite electrolytes are excellent options for use in SSBs due to their structural flexibility and tunability [120]. The remarkable ionic conductivity, stability against air and moisture, and compatibility with lithium metal anodes exhibited by anti-perovskite-type solid electrolytes has attracted significant attention. The structural flexibility and tunability nature of anti-perovskite SEs make them great candidates for use in SSBs [121]. Anti-perovskite solid electrolytes are stable to low-potential anodes and have a very large electrochemical stability window, positioning them as a great option for use in AASSLOBs. Additionally, optimizing the interfaces in anti-perovskite electrolyte-based SSBs can further

improve their performance. Yu et al. [122] developed an in situ “welding” technique to solve the interface problem of the Li<sub>2</sub>OHCl anti-perovskite-type solid electrolyte. A flexible and stable interface was obtained by forming an organic-inorganic compound buffer layer with a one-microliter liquid electrolyte. Figure 4a showcases FESEM, and schematic images illustrate the poor interface between the Li metal and the Li<sub>2</sub>OHCl anti-perovskite-type SE. On the other hand, Figure 4b exhibits FESEM and schematic images depicting the interface’s improvement following the organic welding process.

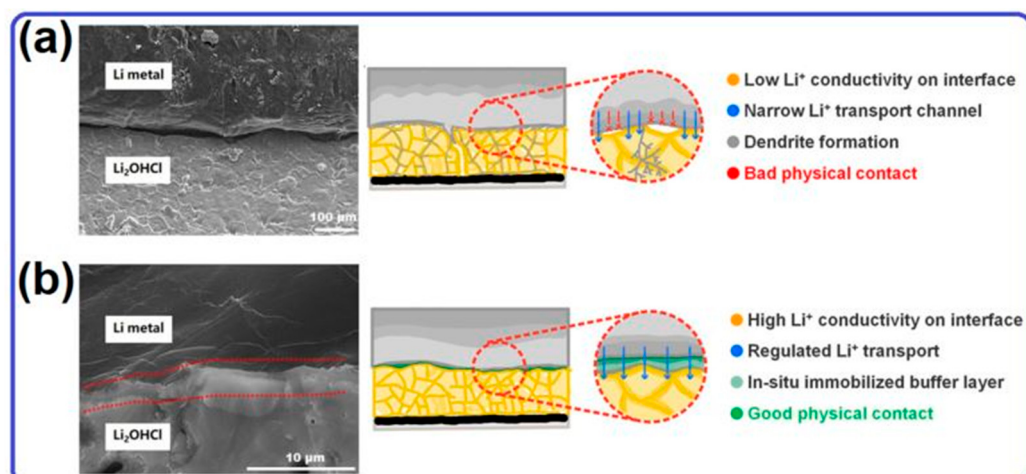


**Figure 4.** (a) FESEM and schematic image illustrate poor interface contact between Li metal anode and Li<sub>2</sub>OHCl SSE pellet. (b) FESEM and schematic image represent enhanced interface contact of Li metal anode with Li<sub>2</sub>OHCl SSE pellet via in situ solidification reaction of liquid electrolyte. Reproduced with permission from Ref. [122]. Copyright 2021, NIH.

Boosting the ionic conductivity of anti-perovskite SEs is also crucial for the advancement of ASSLOBs. Studies have shown that anti-perovskite-type SEs can achieve high ionic conductivity at ambient temperature, with values up to  $10^{-3}$  S cm<sup>-1</sup> [123,124]. Moreover, these electrolytes have demonstrated favorable compatibility with both Li metal anodes and air cathodes, positioning them as promising contenders for ASSLOBs. Nevertheless, additional research is required to enhance the performance and stability of these electrolytes for practical application.

Zeolite-based SEs have received great attention as potential candidates for ASSLOBs owing to their excellent ionic conductivity, thermal stability, and chemical compatibility with the electrodes [125]. Zeolites are porous aluminosilicate materials with a crystalline structure composed of a network of interconnected channels and cavities. These channels and cavities provide pathways for lithium ions to migrate through the solid electrolyte [126,127]. Zeolites provide improved characteristics, such as increased wetting, durability at high temperatures, ion conductivity, strength, and electrochemical stability, compared with conventional solid electrolytes [128].

Recently published studies have presented an integrated ASSLOB design incorporating an ultrathin, high-ion-conductive membrane made of lithium-ion-exchanged zeolite X (LiX) as the electrolyte [41,126]. An encouraging strategy for solid-state Li-Air batteries (SSLABs) entails the in situ combination of LiXZM (Li<sup>+</sup> exchanged zeolite membrane) with cast lithium and carbon nanotubes (CNTs) [41]. This integration resulted in a remarkable ultrahigh capacity of 12,020 mAh g<sup>-1</sup> and an extended lifespan of 149 cycles at a discharge rate of 500 mAh g<sup>-1</sup>, with a limited capacity of 1000 mAh g<sup>-1</sup> in ambient air. Notably, this performance significantly surpassed that of LABs based on LAGP (Li<sub>1+x</sub>Al<sub>y</sub>Ge<sub>2-y</sub>(PO<sub>4</sub>)<sub>3</sub>, lithium aluminum germanium phosphate), which achieved only 13 cycles. The SSLAB with the integrated cathode and LiXZM (referred to as C-LiXZM) demonstrated favorable flexibility and excellent electrochemical performance, offering promising prospects for practical energy storage devices. Zeolites, despite their potential, have certain drawbacks,

including a lack of comprehensive studies, challenges in achieving proper interface contact with electrodes, an increased chance of Li dendrite growth, and issues in large-scale production [129]. Microporous materials, including metal–organic frameworks (MOFs) and zeolites, are intriguing candidates for utilization in composite SEs due to their potential for higher energy density and enhanced safety compared with conventional systems [130]. However, more research is required to comprehensively comprehend the full potential and limitations of zeolite-based solid electrolytes for ASSLOBs.

In summary, SSLOBs are highly regarded as an excellent option for high-performance energy storage. They offer superior safety features by utilizing non-flammable and non-volatile electrolytes. Moreover, these batteries exhibit high specific energy due to the utilization of lithium metal and oxygen gas as active materials. Inorganic solid-state electrolytes for SSLOBs have shown great potential for enabling high energy density, extended cycle life, improved safety, and great chemical stability. Garnet-, perovskite-, anti-perovskite-, and NASICON-type electrolytes have garnered significant attention among the different types of inorganic SSEs. It has been observed that corrosion of the anode, which is one of the difficulties of SSLOBs, can be prevented with inorganic solid electrolytes. Le et al. [131] reported that a perovskite-structured Al-doped Li-La-Ti-O (A-LLTO) SE can significantly improve the stability of LOBs for long-term operation by protecting the lithium anode from O<sub>2</sub>, CO<sub>2</sub>, and humidity in the air.

Moreover, inorganic SSEs can play a crucial role in effectively preventing short circuits resulting from lithium dendrite formation during long-term operation [114,132]. Hybrid quasi-solid-state electrolytes, which merge the benefits of inorganic and organic electrolytes, have also been proposed as a solution for LOBs with increased lifespan and safety [133]. Inorganic solid-state electrolytes are not without drawbacks, including issues including poor ionic conductivity, high interfacial resistance, and limited compatibility with other components of the battery. These limitations highlight the need for continued exploration and innovation in order to overcome these obstacles and boost the overall performance of SSBs.

A hybrid quasi-solid-state electrolyte was proposed as a unique solution for LOBs with extended lifespan and safety [134]. The selection of an inorganic solid-state electrolyte holds substantial influence over the stability, safety, and performance of LOBs. Further research is crucial for the development of novel materials that exhibit enhanced properties in order to address these aspects effectively.

**Organic electrolytes.** Polymer electrolytes have become potential candidates for ASSLOBs owing to their unique properties and advantages. These electrolytes, composed of polymer matrices and lithium salts, offer several benefits, such as better contact with electrodes and excellent mechanical flexibility, compared with inorganic electrolytes. Polymer electrolytes for Li batteries have seen notable advancements across three primary categories: dry solid polymer electrolytes, gel polymer electrolytes (GPEs), and composite polymer electrolytes (CPEs). These developments have contributed to enhanced performance and expanded possibilities for lithium battery technology. However, we will focus on dry solid and CPEs, as gel polymers are not considered in this study. Dry solid polymer electrolytes consist of a polymer host and a Li salt, serving as a solid solvent with no liquid phase. Nonetheless, dry polymer systems often exhibit relatively poor ionic conductivity at ambient temperature, limiting their performance. To address this, composite polymer electrolytes have been shown as a bright strategy. These electrolytes involve incorporating ceramic fillers into the organic polymer host, which effectively lowers the glass transition temperatures and improves the ionic conductivity. This approach enables enhanced performance and conductivity in polymer electrolyte systems.

The fabrication of solid polymer electrolytes (SPEs) typically involves dissolving lithium salts, including Li bisfluorosulfonimide (LiFSI), Li bis(trifluoromethanesulfonyl) imide (LiTFSI), or Li trifluoropotassium sulfonate (LiCF<sub>3</sub>SO<sub>3</sub>), into various polymer hosts. Common polymer hosts employed in SPEs include poly(acrylonitrile) (PAN), poly(ethylene oxide) (PEO), poly(vinylidene fluoride), polyvinylidene fluoride–hexafluoropropylene

(PVDF-HFP), poly(methyl methacrylate), poly(vinyl chloride) (PVC), poly(vinylpyrrolidone) (PVP), and poly(tetrafluoroethylene) (PTFE). Their chemical structures are provided in Figure 5.

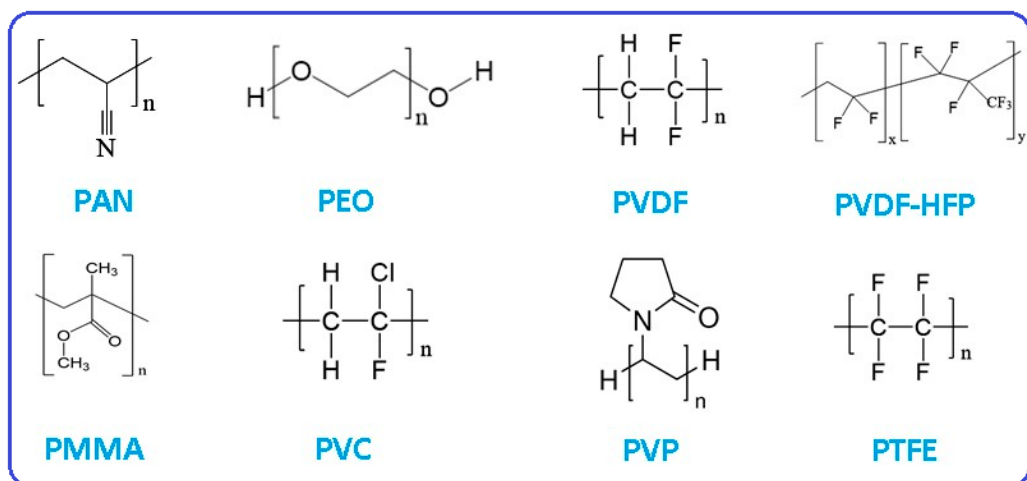


**Figure 5.** The chemical structure of the most common polymers in SEs.

Polyacrylonitrile (PAN)-based polymer electrolytes were among the earliest developed polymer electrolytes. PAN polymers offer many benefits such as chemical stability, non-flammability, thermal durability, and cost-effectiveness [135–137]. However, PAN alone is not typically utilized as a substrate for PEs due to its fragility. To overcome this limitation, PAN can be modified by grafting, copolymerization, or mixing with other polymer monomers that possess high mechanical strength. By incorporating PAN into these ideal polymer electrolyte systems, both the ionic conductivity and mechanical integrity could be enhanced, resulting in enhanced overall performance for various battery applications. The inclusion of -CN groups in PAN facilitates interactions between Li ions and the -CO groups of ethylene carbonate (EC) and propylene carbonate (PC), rendering PAN multifunctional for different applications [138,139].

Tran et al. [140] reported PVA/PAN/LiTFSI/LATP/SN composite polymer electrolytes for ASSLOBs. Figure 6a shows a schematic graphic of the interactions among PVA, PAN, LiTFSI, LATP, and SN. In this study, ionic conductivity ( $1.13 \times 10^{-4} \text{ S cm}^{-1}$ ) and mechanical integrity (Figure 6b) improvability was demonstrated by modifying the PVA polymer electrolyte. The inclusion of -CN groups in PAN facilitates interactions between Li ions and the -CO groups of ethylene carbonate (EC) and propylene carbonate (PC), rendering PAN versatile for various applications. The existence of the -C≡N group in PAN provides strong electronegativity, allowing it to attract Li<sup>+</sup> ions from lithium salts and transition metal ions from cathode materials. Moreover, PAN possesses desirable properties, such as viscosity and oxidation resistance, making it an important polymer for use as a coating layer material. In a study by Chen et al. [141], a solvothermal reaction process was employed to fabricate a thin film coating of PAN on LLZTO particles surface. In Figure 6c, there is a schematic graphic demonstrating the interparticle Li<sup>+</sup> transition within the bulk of the PAN-coated LLZTO electrolyte. A TEM (transmission electron microscopy) analysis was performed to examine and compare the microstructures of PAN-coated LLZTO particles and pristine LLZTO particles. The TEM image revealed that LLZTO particles, with an average size of approximately 100 nm, were enveloped and interconnected by a uniform polymer coating that formed on the particle surfaces (Figure 6d). This resulted in a uniform nanocoating of PAN, which significantly improved the Li<sup>+</sup> transference number to 0.66. Therefore, the thin-film solid electrolyte exhibited a satisfactory ionic conductivity of  $1.1 \times 10^{-4} \text{ S cm}^{-1}$ .

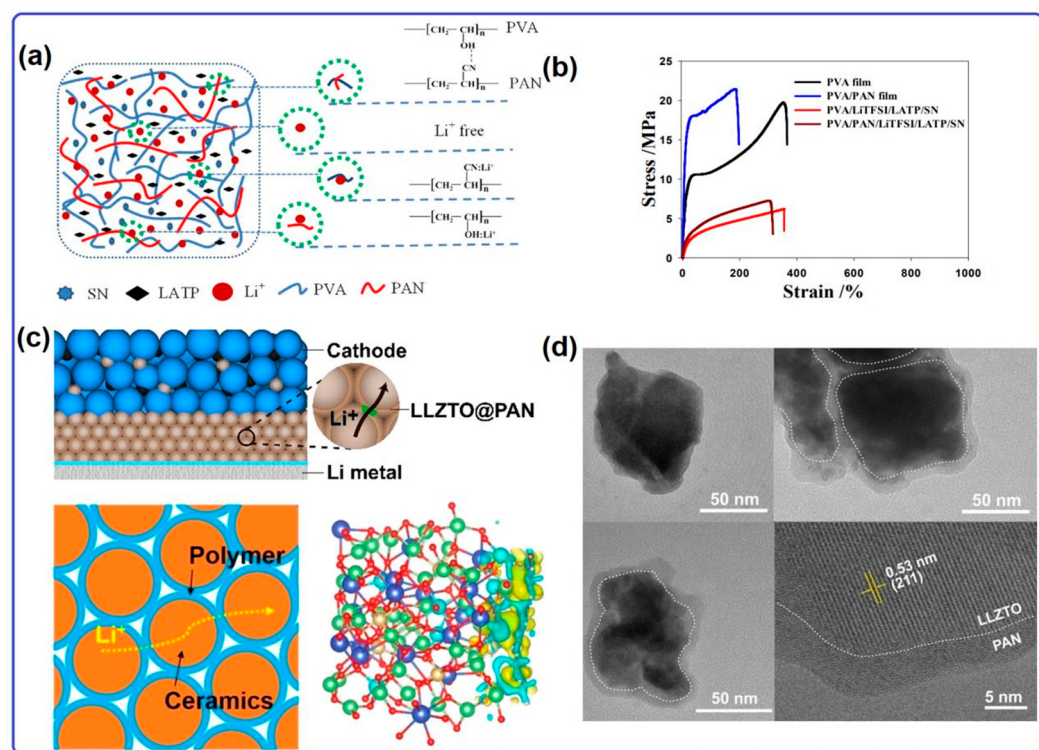


**Figure 6.** (a) Schematic diagram of the interactions among PVA, PAN, LiTFSI, LATP, and SN. (b) Stress–strain curves of a pure PVA film, PVA/PAN film, and PVA/LiTFSI/LATP/SN and PVA/PAN/LiTFSI/LATP/SN SPEs. Reproduced with permission from Ref. [140]. Copyright 2020, American Chemical Society. (c) Schematic pattern shows the interparticle Li<sup>+</sup> transition in the bulk of the composite electrolyte. (d) The TEM images showcase a LLZTO particle in its uncoated form alongside images of LLZTO@PAN particles where the LLZTO particles are connected by a PAN coating. Reproduced with permission from Ref. [141]. Copyright 2021, American Chemical Society.

PEO (polyethylene oxide) has been the subject of significant research in the past two decades as a polymer host for PEs. The investigation of ionic conductivity in PEO electrolyte systems was initiated by Wright in 1975 [142], and Feuillade and Perche explored a polymer plasticization with an aprotic solution composed of alkali metal salts in the same year. PEO is a popular polymer host because of its favorable characteristics, including structural stability, good capacity for salt complexation, high ionic conductivity in the amorphous phase, high corrosion resistance, reasonable cost, flexibility, and chemical durability [143,144]. However, these polymers suffer from limitations such as poor mechanical strength and low ionic conductivity at ambient temperatures (typically in the range of  $10^{-8}$  to  $10^{-7}$  S cm<sup>-1</sup>), which are attributed to the restricted chain motion of PEO [145]. The high crystalline phase of PEO at ambient temperatures hampers ion conduction, resulting in lower ionic conductivity [146]. Above its melting point, PEO-based polymer electrolytes display enhanced conductivity owing to the transition from crystalline to amorphous phases. However, the molten state of PEO results in a loss of dimensional durability and the formation of an extremely viscous liquid, which adversely affects the mechanical resilience of the PEO-based polymer electrolyte matrix. Various strategies have been explored to enhance the ionic conductivity of PEO-based electrolyte systems [147]. The introduction of organic plasticizers and fillers is mainly employed to achieve this. The incorporation of fillers decreases the polymeric crystallinity, leading to improved ionic conductivity. To improve the mechanical stability of PEO-based CPEs, inorganic nanomaterial fillers such as TiO<sub>2</sub>, Al<sub>2</sub>O<sub>3</sub>, and fumed silica have been employed [148,149]. The addition of cyclodextrin into both the polymer matrix and Li salt has demonstrated promising outcomes by enhancing the Li<sup>+</sup> transport in PEO-based polymer electrolytes. This is achieved by weakening the interaction between the ether groups in PEO, facilitating faster Li<sup>+</sup> mobility within the

polymer matrix. Additionally, it creates channels for accelerated Li<sup>+</sup> diffusion from the PEO matrix to LLZTO fillers, enabling faster ion transport. Furthermore, a new method was devised by He et al. [150], which utilized the intermolecular interaction between ethylene carbonate (EC) and Ta-doped LLZO Li<sub>7</sub>La<sub>3</sub>Zr<sub>2</sub>O<sub>12</sub> (LLZTO) in P(EO)<sub>15</sub>LiTFSI, as depicted in Figure 7a. The LLZTO-induced ring opening reaction of EC leads to the formation of oligomers with ether oxygen chains, providing an additional pathway for efficient Li<sup>+</sup> conduction. Furthermore, EC acts as a disruptor to the PEO chain, expanding the amorphous phase region and facilitating Li<sup>+</sup> migration. Consequently, the PEO-based electrolyte achieves a room temperature conductivity of  $1.43 \times 10^{-3}$  S cm<sup>-1</sup> (Figure 7b).

Another strategy involves blending PEO with other polymers, such as PMMA, to enhance the ionic conduction of PEO-based systems. The flexible backbone and amorphous nature of PMMA contribute to a reduction in the mechanical strength of PEO, allowing for improved ionic conduction [151]. Another effective additive for solid-state batteries is succinonitrile (SN), which also contains cyano groups. The -C≡N groups in SN have the ability to incorporate with a Li salt and other polymers. In the case of PEO-SN systems, they can establish a fast pathway for Li<sup>+</sup> movement, even in the absence of a lithium salt. An analysis of NMR spectra conducted by Xu et al. [145] revealed that the incorporation of a high content of SN (SN:EO = 1:4) can promote the formation of fast ion channels, resulting in the development of homogeneous SSEs, as depicted in Figure 7c.

Extensive research has been dedicated to the synthetic development of PEO-based solid polymer electrolytes for ASSLOBs, including copolymerization, crosslinking, and hyperbranching [152,153]. In a study carried out by Wang et al. [154], a solution-casting technique was utilized to crosslink a hydrolyzed polymaleic anhydride (HPMA) low-molecular polymer plasticizer with PEO and Li salt, as shown in Figure 7d. The physical entanglement between HPMA and PEO, as well as the presence of the -COOH group on HPMA, played a critical role in decreasing the crystallization and promoting the amorphous phase of PEO. This structural modification resulted in an enhancement in the ionic conductivity of the PEs.

Overall, PEO-based PEs are a potential avenue for the advancement of ASSLOBs, and research efforts are ongoing to improve their performance and stability.

PVDF has gained significant consideration in the improvement of lithium batteries owing to its excellent properties, such as a strong affinity to electrolyte solutions, excellent electrochemical durability, and high dielectric constant [155]. The existence of CF groups in PVDF chains contributes to the wide electrochemical stability range of the polymeric solid electrolyte, which can be up to 4.5 V or higher [156]. However, despite these favorable characteristics, the mechanical strength of PVDF-based electrolytes remains insufficient for practical applications [157,158]. Several strategies can be utilized to increase the mechanical features and suitability of the electrolyte for real-world applications. These approaches include incorporating reinforcing fillers or blending PVDF with other polymers, which effectively improve the mechanical performance of the electrolyte [159].

PVDF polymers indicate a high degree of crystallinity, which can affect their performance in Li-based systems. The inclusion of fluorine (-F) in the PVDF chain makes it susceptible to reactions with lithium metal, particularly during repetitive charge and discharge cycles. This reaction results in a reduction in the hydrophobicity of the membrane, allowing moisture from the air to penetrate and potentially damage the Li negative interface. To address these challenges, researchers have explored the use of PVDF-HFP membranes with oxygen selectivity. A copolymer of PVDF-HFP consists of two distinct monomers: symmetrical vinylidene fluoride (VdF) and asymmetrical hexafluoropropylene (HFP) [160]. This unique combination of crystalline PVDF and amorphous HFP in the copolymer results in a high ionic conductivity and good mechanical resilience [161]. PVDF, with its high degree of crystallinity, exhibits relatively lower conductivity. However, when combined with the PVDF-HFP host, which comprises two randomly mixed monomers, the resulting film allows for improved mobility of free lithium ions and higher amorphicity, resulting in improved conductivity [158,162]. PVDF-HFP has emerged as a highly suc-

cessful matrix for polymer electrolytes in LOBs, serving as one of the key materials in this application [163]. PVDF-HFP-based polymer electrolytes with high  $\text{Li}^+$  transference numbers have been studied to enhance the cycling stability and rate capability of lithium metal batteries (LMBs) [164,165]. The detailed discussion of hybrid polymer electrolytes for LOBs encompassed various compositions, focusing on crucial aspects such as electrolyte conductivity and stability.

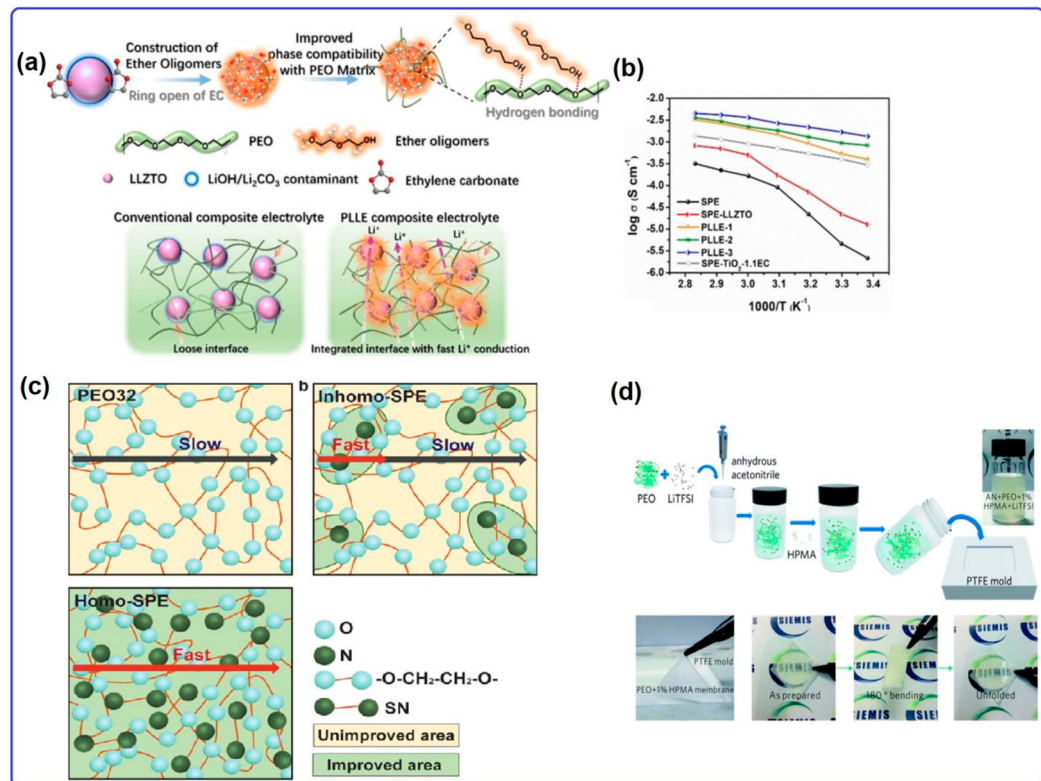


**Figure 7.** (a) The intermolecular interaction mechanism between  $\text{LiOH}/\text{Li}_2\text{CO}_3$ -contaminated LLZTO and EC in PEO-based composite electrolytes. (b) Arrhenius plots of PEO and its composite electrolytes. Reproduced with permission from Ref. [150]. Copyright 2021, Wiley. (c) Carbon conformation transition graphic and  $\text{Li}^+$  transport modes of PEO and SN–PEO SPEs. Reproduced with permission from Ref. [145]. Copyright 2020, Wiley. (d) Schematic of the PEO-HPMA SPE-based all-solid-state Li-metal battery. Reproduced with permission from Ref. [154]. Copyright 2020, Royal Society of Chemistry.

PMMA-based polymer electrolytes are derived from methyl methacrylate (MMA) or methyl propionate (MA). These PEs present numerous advantages, including a broad electrochemical stability range exceeding 4.5 V, excellent room temperature ionic conductivity ( $10^{-3}$  S cm<sup>-1</sup>), and favorable compatibility with both positive and negative electrodes [166]. However, PMMA-based PEs often undergo low mechanical integrity and high brittleness [167,168]. To address this issue, PMMA is often used in combination with other substrate materials to harness its desirable properties while improving mechanical strength. By incorporating PMMA into CEs or utilizing it as a component in polymer blends, the overall performance and mechanical strength of the electrolyte system can be improved. Ramesh and Liew [166] revealed an enhancement in ionic conductivity by blending PMMA with PVC and doping it with the LiTFSI lithium salt. Numerous studies have been dedicated to optimizing the properties and performance of PEs based on PMMA using different additives and mixing techniques [165]. Overall, PMMA-based PEs are a potential avenue for the improvement of ASSLOBs, and research efforts are ongoing to improve their performance and stability. However, additional studies are required to ascertain the specific advantages of PMMA-based polymer electrolytes for ASSLOBs [47,133,169,170].

Poly(vinyl alcohol) (PVA) has been studied as an SPE for Li batteries [140,171]. It possesses a range of desirable characteristics, including good elasticity strength, mechanical resilience, eco-friendliness, low cost, good optical characteristics, high temperature stability, and a high level of hydrophilicity [172,173]. The hydrophilicity of PVA is attributed to the abundance of polar hydroxyl groups within its structure. In addition to these properties, PVA offers advantages such as ease of production, high erosion resistance, good elasticity, biocompatibility, and high chemical and thermal durability [174,175]. PVA holds promise as a versatile and functional host polymer for various electrochemical applications.

The advancement of PEs for ASSLOBs is still an active research area. Despite the presence of certain limitations in SPEs, including poor lithium ionic conductivity due to crystallizing and the potential decomposition of the polymer matrix in open operating atmospheres, their high tolerance to battery volume changes and excellent processability make them highly promising for the development of flexible SSLOBs. Researchers are actively working on developing polymer electrolytes with enhanced lithium-ion conductivity through various strategies such as optimizing polymer composition, incorporating additives, and improving polymer morphology. Another challenge is the stability of the PE in the presence of Li and oxygen. The highly reactive nature of lithium and oxygen can cause degradation and decomposition of the polymer electrolyte, leading to a decrease in battery performance over time. Research efforts are focused on designing polymer electrolytes with improved stability and compatibility with lithium and oxygen to ensure long-term operation of ASSLOBs. Furthermore, the interface of PE and the electrode materials is vital for efficient charge and ion transport. To enhance the overall performance of ASSLOBs, it is crucial to focus on the improvement of interfacial engineering approaches and a deeper understanding of interfacial phenomena. While notable progress has been achieved in the development of polymer electrolytes for ASSLOBs, there are still technical challenges that must be overcome before they can be effectively commercialized. Further research and development efforts are required to enhance the Li ion conductivity, stability, and interface properties of PEs for ASSLOBs.

**Composite Electrolytes.** In LOBs, ceramic electrolytes show ideal Young's modulus, good ionic conductivity ( $>10^{-4}$  S cm<sup>-1</sup>) and thermal durability, and superior conductivity, while polymer electrolytes provide good wetting, lightness, and improved flexibility [176]. However, the high temperature treatment used to produce ceramic electrolytes results in inadequate contact of the ceramic electrolyte with the electrode, which increases the interfacial resistance [177]. In polymer solid electrolytes, there are problems of poor interface contact and low ionic conductivity entailing the crystallinity of the polymer matrix and low chain movement at room temperature [178]. There is an increasing interest in composite electrolytes that merge the benefits of these two electrolytes and eliminate their disadvantages. Inorganic ceramic electrolytes are utilized primarily as fillers in composite solid electrolytes (CSEs) to enhance both the mechanical strength and ionic conductivity. Polymer matrices used in CSEs reduce the electrode–electrolyte interface resistance, increase the flexibility, and provide an easy production process [179]. Some features should be considered when designing composite electrolyte for LOBs. The composite solid electrolyte used in LOBs should be stable after contact with O<sub>2</sub>. It should also consist of hard inorganic components with 3D ion transport channels that evenly cover the Li anode surface to ensure an even distribution of Li<sup>+</sup> ions and high mechanical strength. Composite solid electrolytes should possess a smooth surface, while maintaining sufficient flexibility to establish close contact with the electrodes [180].

In the study by Ouyang et al. [181], high-shear garnet oxide electrolyte Li<sub>6.75</sub>La<sub>3</sub>Zr<sub>1.75</sub>Ta<sub>0.25</sub>O<sub>12</sub> (LLZTO) and non-ionic and high polarity solid organic plastic crystalline succinonitrile (SN) formed a composite solid electrolyte. They mixed LiTFSI salt with poly(vinylidene fluoride-co-hexafluoropropylene) (PVDF-HFP), an attractive modified polymer with favorable electrochemical stability at ambient temperature, relatively poor crystallinity, and a high dielectric constant, which is used as an additive in electrolytes, providing thermal stability owing to its high boiling point and low vapor pressure prop-

erties. Thanks to the high polarity of SN, which proves to be able dissolve different salts including LiTFSI, the ionic conductivity of the CSE can increase up to  $10^{-3}$  S cm $^{-1}$  at room temperature. In addition to the mentioned properties of SN, it accelerates the passage of Li ions in the solid electrolyte by lowering the energy barrier. The ASSLOB prepared with the LLZTO-SN electrolyte showed low resistance at room temperature, a large discharge capacity ( $>9500$  mAh g $^{-1}$ ), high rate capability, and a stable long cycle life. Song et al. [177] produced a Li<sub>7</sub>La<sub>3</sub>Zr<sub>2</sub>O<sub>12</sub> (LLZO) garnet filler within a polystyrene (PS) latex microsphere template. The polyethylene oxide (PEO) matrix was later incorporated into the structure, resulting in the formation of 3D and macroporous composite polymer electrolytes, as illustrated in Figure 8a. Figure 8b illustrates the well-defined spherical morphology of the PS particles, exhibiting an average diameter of 1.37  $\mu$ m and a narrow size distribution. The SEM images in Figure 8c reveal the presence of three-dimensional (3D) LLZO grains with macropores that can accommodate the PEO matrix and prevent crystallization of the polymer. These LLZO grains exhibit a grain size ranging from 1 to 3  $\mu$ m and possess a smooth surface, facilitating rapid ion transport through the continuous interfaces of the PEO matrix with the LLZO framework. The smooth and dense 3D composite polymer electrolyte, depicted in Figure 8d, exhibits a uniform surface without any voids. Furthermore, the cross-sectional view in Figure 8e indicates that the composite electrolyte has a thickness of approximately 200  $\mu$ m. Figure 8f demonstrates the preservation of the 3D-LLZO structure within the PEO matrix, revealing the presence of pores that facilitate the transport of Li $^{+}$  ions. The digital photographs depicted in Figures 8g and 2h demonstrate the remarkable flexibility of the composite polymer electrolyte, exhibiting no indications of cracking or breaking, even when subjected to bending and folding. The 3D PEO-LLZO composite polymer electrolyte demonstrates remarkable stability, retaining its morphology and structure consistently, even after prolonged cycling. This exceptional stability safeguards both the anode and cathode, even under challenging reducing and oxidative conditions. The 3D LLZO networks obtained using PS template provide good interfacial and mechanical compatibility in PEO matrix structure while widening the ionic conduction path. The XRD graph presented in Figure 8i clearly illustrates that even after undergoing 50 cycles, the structures of both the anode and cathode components of the electrolyte remain intact, with no formation of impurities observed. These findings indicate the exceptional stability of the 3D composite polymer electrolyte when in contact with the reducing Li metal anode, effectively resisting the oxidative attack from active oxygen species and O<sub>2</sub>. The stability of the 3D CPEs meets the essential requirements with remarkable efficacy.

Although NASICON-type Li<sub>1.5</sub>Al<sub>0.5</sub>Ge<sub>1.5</sub>(PO<sub>4</sub>)<sub>3</sub> (LAGP) serves as a promising ceramic electrolyte in SSLOBs, it is important to avoid direct contact between Ge $^{4+}$  and the Li metal. Direct contact can cause the reduction of Ge $^{2+}$  and Ge0 by the lithium metal, resulting in the deterioration of the crystal structure, reduced Li ion conductivity, and increased interfacial impedance during the electrochemical processes. In order to create a stable interface layer between the Li metal and LAGP, Wang et al. [180] designed a CSE by adding a small quantity of PVDF-HFP with nanosized ceramic LAGP electrolyte. By employing an ultrathin and flexible shell of PVDF-HFP, the Li metal establishes a soft contact with the LAGP core. This arrangement effectively suppresses the reduction of Ge $^{4+}$  that can occur when Ge $^{4+}$  directly interacts with the lithium metal. The hybrid solid electrolyte (HSE) formation caused dendrite-free Li deposition, primarily attributed to the core–shell interface. Three comparison groups were studied: HSE-I utilizing micro-size LAGP; HSE-II incorporating nanometer-size LAGP with low LAGP content; and GPEs without LAGP, which were prepared to conduct a detailed investigation of the proposed HSE using nanoscale LAGP and to observe the functionality of the core–shell interface. Figure 9a exhibits the comparison of the lithium deposition mechanism of three various HSEs and GPEs. Accordingly, in the HSE used in LOBs, the thin flexible polymer shell provides homogeneous Li $^{+}$  distribution and almost prevents dendrite formation on the Li sheet. However, the rough surface caused by the microsized LAGP grains used in HSE-I causes rapid depletion of ions in the area that is not locally in contact with the Li sheet.

As a result,  $\text{Li}^+$  accumulates uniformly during nucleation, while dendrites are formed in the later growth stage. LAGP, which is used in an insufficient amount in HSE-II, forms dendrites during the nucleation process. On the contrary, in the case of GPE, the non-uniform distribution of lithium ions can result in the continuous formation of dendrites, leading to the rapid perforation of the GPE. Figure 9b displays the SEM images of the Li layer after use in four different electrolytes. Except for some cracks, no dendrites were identified in the lithium layer using the HSE electrolyte. After cycling, a few spherical dendrites were observed in the Li plate containing HSE-I, which utilized microsized LAGPs. This occurrence can be assigned to the irregular distribution of the microparticles within the lithium ions. Insufficient  $\text{Li}^+$  content leading to local disorder resulted in more pronounced dendrite formation in the  $\text{Li}-\text{O}_2$  cell using HSE-II, which incorporated a small quantity of nanosized LAGP. The presence of a high proportion of ultrathin, soft layers contributed to the diminished electrochemical performance in the cell. Similar to the cell utilizing HSE-II, the cell with GPE experienced the formation of a substantial and porous dendrite layer that covered the Li plate surface, leading to an inadequate electrochemical performance. Figure 9d illustrates that the composite solid electrolyte obtained by using a polymer on a ceramic matrix maintains its structural integrity, even at high temperatures, compared with GPE.

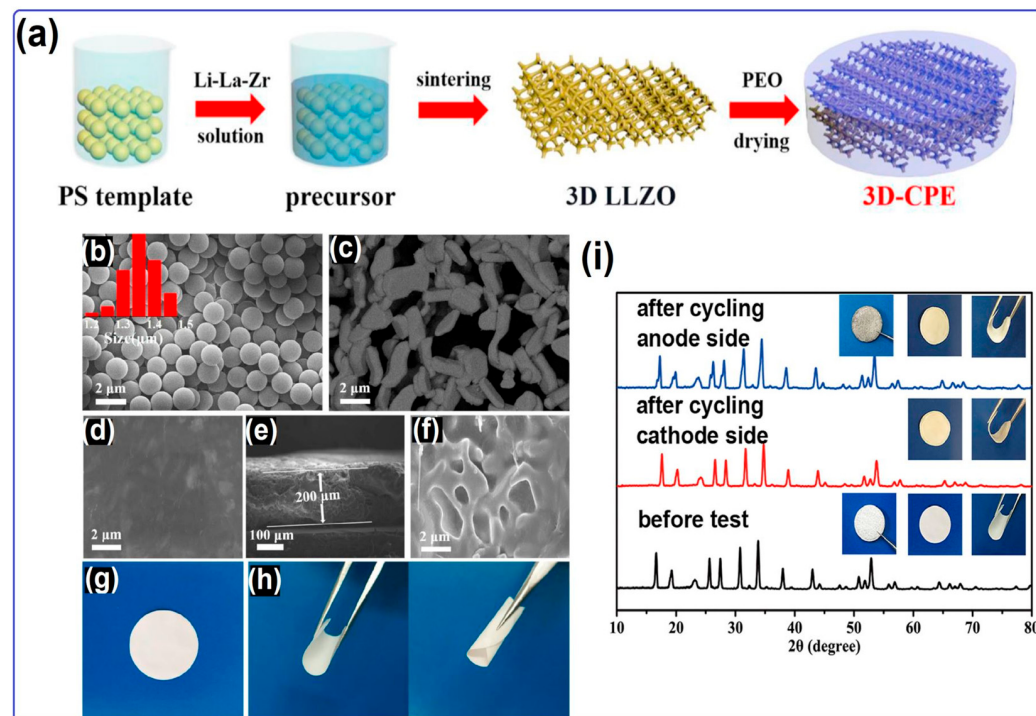


**Figure 8.** (a) Schematic illustration of the production process for PEO/LLZO CPE, SEM images of PS microsphere templates (b), 3D LLZO network grains (c), and the surface (d) and cross section of 3D-CPE in low (e) and high (f) magnification, digital photos of 3D-CPE discs at flat (g) and bent states (h). (i) XRD patterns of 3D PEO/LLZO electrolyte surface before and after 50th cycle. Reproduced with permission from Ref. [177]. Copyright 2020, Elsevier.

Designing a solid electrolyte is complicated because of the porous structure of the solid electrolyte and the requirement for high electronic and ionic conductivity. A typical solid electrolyte comprises multiple solid-state interfaces, which include the interface between the discharge residue and the ionic conductor, as well as the interface between the discharge residue and the electronic conductor [182]. It is crucial for the ionic conductor and electronic conductor to establish compact contact to facilitate efficient electron/ion exchange in the solid electrolyte and to assist in the formation and decomposition of the discharge products [183,184]. Zhaou et al. [185] obtained composite solid electrolyte

with 3D porous garnet microstructure electrolytes with a GPE. While forming the solid composite electrolyte, poly(methyl methacrylate) (PMMA) nanospheres were utilized as scaffolds to form the pores. In their study, LLZTO was utilized as the ceramic electrolyte, PVDF-HFP served as the gel polymer electrolyte, and LiClO<sub>4</sub> was employed as the salt. The preparation procedure is depicted in Figure 10a. The SEM images in Figure 10b–f reveal that the composite electrolyte, prepared with a combination of a porous solid electrolyte (PSSE) and GPE, exhibits a range of pore sizes between 10 and 100 µm. The composite electrolyte, formed by the close contact between the PSSE frame and the GPE, enables the fast movement of Li<sup>+</sup> ions between the two components, ensuring efficient ion conductivity. Lithium-ion transport of the composite electrolyte throughout the entire matrix is advantageous for enhanced ionic conductivity. In Figure 10g, consecutive GPEs with high ionic conductivity serve as “sail pathways”, enabling rapid and dense Li-ion transport. Meanwhile, the PSSE framework with moderate ionic conductivity acts as “walking pathways”, facilitating the additional source of Li-ion to traverse the intricate routes and complete the overall transport process. An ionic conductivity value of  $1.06 \times 10^{-3}$  S cm<sup>-1</sup> was obtained from the CSE. This value is almost competitive with GPE ( $3.48 \times 10^{-3}$  S cm<sup>-1</sup>), while it is almost 4 times greater than ceramic electrolyte ( $2.0 \times 10^{-4}$  S). As shown in Figure 10h–j, after 25 cycles, the lithium anode with PSSE/GPE electrolyte has a nearly smooth surface, with no exfoliated particles visible on the surface. Figure 10k,m show the presence of numerous waste Li particles on the surface of the lithium with the GPE. Accumulation of waste Li with GPE on the Li metal anode surface causes high polarization, reducing the electrochemical stability of the cell. The LLZTO/GPE composite electrode showed a capacity value of almost 1250 mA h g<sup>-1</sup> for 200 cycles, while the GPE showed this value by operating for 31 cycles. The 3D garnet microstructure acted as a solid constituent for mechanical support and lithium dendrite prevention. The GPE in the 3D frame provided density in the structure and prevented the O<sub>2</sub> transition, thus providing a high ionic conductivity.

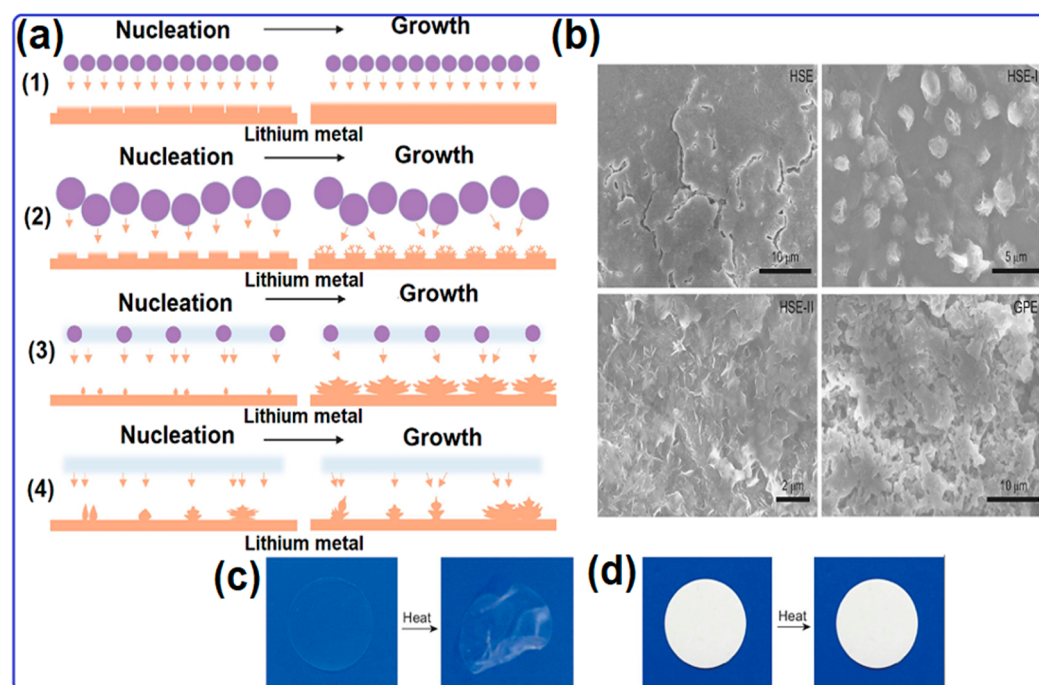


**Figure 9.** (a) Diagram illustration of lithium deposition with (1) HSE, (2) HSE-I, (3) HSE-II, and (4) GPE. (b) SEM images were obtained by disassembling lithium sheets from symmetric cells applied to cycling tests with different electrolytes, namely HSE, HSE-I, HSE-II, and GPE. (c) GPE and (d) HSE before and after heating at 150 °C for 5 min. Reproduced with permission from Ref. [180]. Copyright 2021, Oxford University.

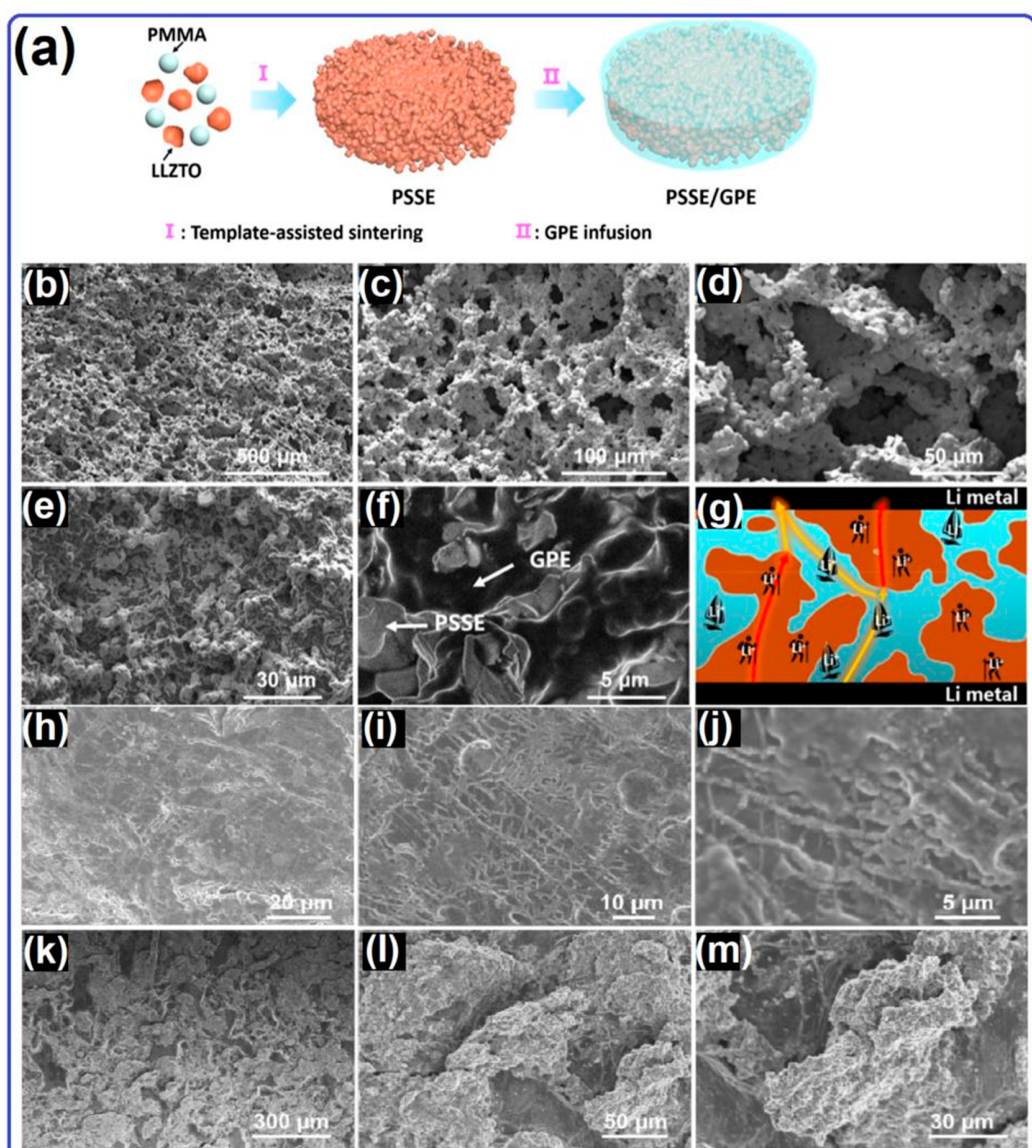


**Figure 10.** (a) Schematic illustration depicts the preparation of PSSE/GPE, and SEM images display the as-prepared PSSE (b–d) and (e,f) PSSE/GPE. (g) Schematic representation of Li-ion transportation in PSSE/GPE. SEM micrographs of Li metal after 25 cycles with (h–j) PSSE-GPE and (k–m) GPE electrolytes. Reproduced with permission from Ref. [185]. Copyright 2020, American Chemical Society.

GPEs, which are produced by adsorbing liquid electrolytes in the polymer matrix, find applications in LOBs because they have the properties of both solid and organic liquid electrolytes. The flexible structure of GPEs can suppress the volumetric change of the electrode during the electrochemical process, and its gel property facilitates  $\text{Li}^+$  diffusion [186]. Ceramic fillers are added to GPEs to increase their mechanical strength and ionic conductivity. Cations in the structures of ceramic fillers act as Lewis acids. These cations take the place of  $\text{Li}^+$  by reacting with  $\text{O}_2$  or other functional groups in the polymer [187]. Thus, the recrystallization of the polymer is prevented, and the Li salts are easily separated. Oxygen in ceramic fillers acts as a Lewis base. The oxygen in the structure interacts with  $\text{Li}^+$  and forms a  $\text{Li}^+$ -rich state at the filler/polymer interface, acting as a new pathway for lithium-ion transition. As a result, there is an increase in the number of  $\text{Li}^+$  transported [188]. Liu et al. [170] designed composite GPE using poly(methyl methacrylate)(PMMA) and  $\text{SiO}_2$  and using LTFSI as a salt for ASSLOBs.  $\text{SiO}_2$  added to GPE prevents polymer recrystallization, and the interaction between  $\text{Li}^+$  ions and  $\text{OH}^-$  groups on the  $\text{SiO}_2$  surface favors the formation of a lithium-ion migration pathway.

The composite electrolytes offer a solution to the issues found in ceramic and polymer electrolytes for ASSLOBs. Composite electrolytes can improve ionic conductivity and prevent dendrite formation at the anode by creating porous structures, reducing grain size, and incorporating conductive fillers. Additionally, appropriate fillers can reduce polarization on the cathode side and improve overall electrochemical performance. Furthermore, the flexibility of composite electrolytes can protect both the anode and cathode, thereby minimizing volumetric expansion problems. The properties of some recent solid electrolytes and their performances in LOBs are given in Table 2.

**Table 2.** The performance of lithium–oxygen cells prepared with various solid electrolytes.

Solid-State Electrolytes	Ionic Conductivity ( $\text{S cm}^{-1}$ )	Li Transfer Number	Li Salt	Cycle Number	Ref.
LATP	$7 \times 10^{-4}$	-	-	100	[189]
LATP	0.71	-	-	50	[190]
LATP	-	-	-	1174	[191]
LATP	$5.23 \times 10^{-4}$	-	-	200	[192]
LAGP	$3.9 \times 10^{-4}$	-	-	27	[182]
LAGP	$2 \times 10^{-4}$	-	-	20	[40]
LAGP	$4.5 \times 10^{-4}$	-	-	80	[193]
LAGP/LiT <sub>2</sub> O <sub>3</sub>	-	-	-	59	[194]
LAGP/Li <sub>3</sub> InCl <sub>6</sub>	$13 \times 10^{-4}$	-	-	33	[184]
Al-doped LLTO/PVDF-HFP	$3.17 \times 10^{-4}$	-	LiTFSI	132	[115]
LLZTO	$16 \times 10^{-4}$	-	PPC:LiTFSI	50	[195]
LLZTO	$16 \times 10^{-4}$	-	-	5	[196]
LLZT-xAl <sub>2</sub> O <sub>3</sub>	-	-	-	43	[197]
LiXZM	$2.67 \times 10^{-4}$	-	-	149	[41]
Poly (methyl methacrylate)	$2.5 \times 10^{-2}$	0.47	LiTFSI	-	[198]
Polyimide	0.44	0.596	LiTFSI	156	[199]
SN/LiTFSI/P(VDF-HFP)/BHT	$3.87 \times 10^{-4}$	-	LiTFSI	130	[200]
PEO/LiBETI/Li <sub>2</sub> O/BN/LAGP	-	-	LiBETI/Li <sub>2</sub> O	40	[201]
PEO/LiT <sub>f</sub>	-	-	LiT <sub>f</sub>	40	[202]
P(VDF-HFP)/LiFSI	$0.79 \times 10^{-4}$	-	LiFSI	60	[203]
LLZTO/SN	$2.73 \times 10^{-4}$	0.48	LiTFSI	60	[181]
LLZO/PS	$9.2 \times 10^{-5}$	-	LiTFSI	50	[177]
LAGP/PMS	$3.2 \times 10^{-4}$	0.75	LiTFSI	160	[204]
PVDF-HFP/Ti <sub>3</sub> AlC <sub>2</sub>	$5.45 \times 10^{-4}$	0.47	LiTFSI	200	[205]
SiO <sub>2</sub> /PIB	$9.1 \times 10^{-4}$	-	LiTFSI	150	[206]
PVDF-HFP/SiO <sub>2</sub>	$9.3 \times 10^{-4}$	-	LiTFSI	89	[207]

### 2.3. Cathode Architecture for Solid-State Lithium–Oxygen Batteries

As an alternative to LOBs that use volatile and explosive organic liquid electrolytes, the development of ASSLOBs shows significant promise. However, because of the weak

ionic conductivity of SEs, the considerable interfacial resistance, and the restricted reaction sites of cathodes, the implementation of high-performance SSLOBs is a challenge. The development of an ideal cathode for ASSLOBs has been impeded practically by a limited capacity and short cycle life. For the air cathode to effectively accommodate the deposition and decomposition of the discharge products, it necessitates a high porosity structure, excellent electronic conductivity, and high catalytic activity for both oxygen reduction and oxygen evolution reactions [208]. Unfortunately, the generation and dissolution of the discharge residue ( $\text{Li}_2\text{O}_2$ ) in two-electron processes have slow reaction rates. The ASSLOBs typically lead to large discharge overpotentials and poor Coulombic efficiencies due to the low electrochemical reversibility of  $\text{Li}_2\text{O}_2$ . Furthermore, the high interfacial resistance between the cathode and the SE hindered the reaction rates. As a result, developing a highly effective catalyst is a “significant issue” for ASSLOBs. Carbon-based materials are frequently chosen as catalysts, as is well known owing to their remarkable catalytic activity, light weight, superior conductivity, and enriched porous structure. It appears that carbon-based materials with nanostructures can efficiently improve the electrochemical kinetic reaction.

In contrast, the organic electrolytes in current aprotic LOBs are easily decomposed by the strong oxidative radicals generated at the cathode, resulting in poor cyclability. Recently, solid-state cathodes composed of stable ceramic electrolytes rather than organic electrolytes have been designed to address this issue. These cathodes offer a capacity by formation of  $\text{Li}_2\text{O}_2$  via an electrochemical reaction among the lithium ions,  $e^-$ , and oxygen, although, due to the weak electron/ion transport in  $\text{Li}_2\text{O}_2$  and the lack of a liquid medium for  $\text{Li}_2\text{O}_2$  development, the formation of  $\text{Li}_2\text{O}_2$  particles within the solid-state cathode is constrained. Consequently, the capacity of LOBs with a solid-state cathode is inherently restricted. To circumvent the restriction caused by the low growth of the  $\text{Li}_2\text{O}_2$  particles within the solid-state cathode, it is possible to develop an environment that promotes the expansion of the discharge product. According to a study by Kim et al. [209], the discharge product can be converted from growth-restricted  $\text{Li}_2\text{O}_2$  to easily produced LiOH by adding water steam to the oxygen used in the SSBs (Figure 11), and a ruthenium-based composite that conducts both electronically and ionically was developed as a solid-state cathode. The pouched cathode film was attached to an LATP plate to assemble an ASSLOB cell, and the cells demonstrated a high stability over 665 cycles. This strategy offers new perspectives on designing effective ceramic-based solid-state cathodes for feasible LOB systems.

Additionally, the integrated structure design for ASSLOBs has drawn more interest because it has proven to have high potential, even at a broad range of room temperatures (up to 120 °C). In our previous work, we developed an integrated structure cathode by coating GPE on a  $\text{MnO}_2/\text{Ru}$  nanowire hybrid framework [210], which established a compact interfacial contact between the GPEs and the cathode. The air cathode, utilizing the advantages of its 3D porous nanowire structure, can provide a sufficient number of active sites for catalytic reactions, such as oxygen reduction and oxygen evolution reactions. Furthermore, this structure helps to minimize resistance related to charge transfer and mass diffusion, thereby enhancing overall performance. The ASSLOB cells also provides a high specific capacity of 14,384 mAh g<sup>-1</sup> at 200 mA g<sup>-1</sup>. In a recent study, a flexible integrated cathode–electrolyte structure was developed with the aim of establishing a robust interaction between the cathode and electrolyte. This was achieved by anchoring them onto a three-dimensional  $\text{SiO}_2$  nanofiber structure.

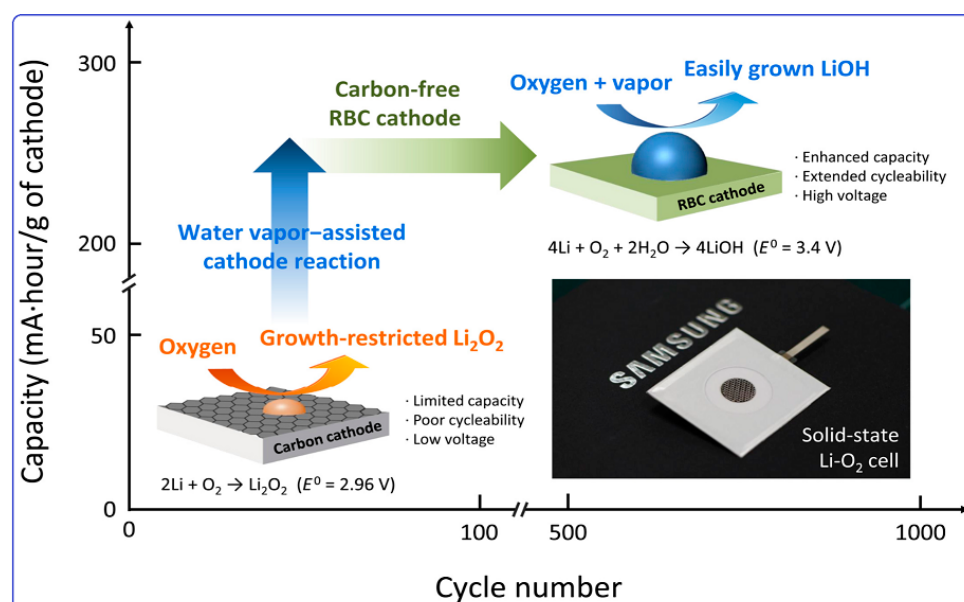


**Figure 11.** Experimental investigation of the effects of adding water vapor to a dry O<sub>2</sub> atmosphere on the discharge performance of an ASSLOB cell with a ruthenium-based cathode. Reproduced with permission from Ref. [209]. Copyright 2022, Science.

The development of a carbon-coated porous Li<sub>1.5</sub>Al<sub>0.5</sub>Ge<sub>1.5</sub>P<sub>3</sub>O<sub>12</sub> (LAGP) layer through straightforward one-step annealing was reported by Zhou et al. [211]. An effective integrated design can potentially lower interface resistance and promote the electrochemical performance of the cell. Li et al. [212] proposed using a 3D SiO<sub>2</sub> nanofiber (NF) membrane to develop a flexible integrated cathode–electrolyte structure (ICES) for ASSLOBs. The SiO<sub>2</sub> NFs framework acts as a bridge connecting the composite solid electrolyte (CSE) and cathode, improving ionic conductivity and reaction sites. The ICES exhibits a high discharge capacity (9220 mAh g<sup>-1</sup>), rate capability, and cycle lifetime (145 cycles). The CSE also inhibits the dendrite growth and increases the battery safety. The ICES-based SSLOBs demonstrate lower resistance and improved performance compared with carbon-based ASSLOBs.

The field of ASSLOBs is continually advancing, and researchers are actively investigating different cathode materials and configurations to tackle the challenges related to stability, reversibility, and efficiency. Ongoing research and development endeavors are crucial to overcome these obstacles and unlock the complete potential of ASSLOBs.

### 3. Machine Learning of All-Solid-State Lithium Batteries

All-solid-state lithium–oxygen batteries offer significant potential for advanced technologies, such as digitization and ML in terms of battery performance and management [213]. Digitization refers to various data collection and analysis methods used for the monitoring, control, and optimization of LOB performance. Data obtained from the battery through sensors and data acquisition devices can be utilized to understand the battery's state and behavior [214]. This enables enhanced performance, efficiency optimization, and extended lifespan. Digitization also holds benefits in areas such as battery prognosis, fault detection, and energy management.

Machine learning can be a valuable tool for ASSLOBs. Machine learning algorithms can be employed to model and predict the complex performance characteristics and responses of batteries. This aids in optimizing energy storage capacity, managing charge/discharge rates, performing fault diagnosis, and predicting battery lifespan [215]. ML models can be updated and adapted in real-time to enhance battery performance and optimize energy efficiency. However, it should be noted that digitization and ML are still evolving areas in the field of fully solid-state lithium–oxygen batteries. Challenges such

as data collection, data reliability, and model training need to be addressed. Additionally, important aspects such as battery safety, performance, and sustainability should be taken into consideration.

There has been a growing interest in the digitalization and ML efforts for SE materials in recent years [216]. Digitalization efforts aim to create large databases that contain information on various material properties, such as crystal structure, electronic structure, ionic conductivity, and electrochemical stability. These databases can then be used to develop ML models that can predict and optimize the properties of the SE materials. ML techniques can be applied to SE material data in several ways:

**Data generation and analysis.** ML algorithms can be used to generate large datasets of SE material properties, such as conductivity, stability, and electrochemical performance. These algorithms can also analyze existing datasets to identify patterns and correlations among different material characteristics.

**Property prediction.** ML models can be trained to predict various properties of SE materials based on their composition, crystal structure, and other factors. These models can provide valuable insights into the behavior of these materials and help researchers design new materials with the desired properties.

**Material discovery and optimization.** ML can be used to accelerate the discovery and optimization of SE materials. By analyzing large amounts of data on material synthesis and performance, ML algorithms can guide researchers towards promising candidates for further investigation.

**Property–structure relationships.** ML techniques can help establish relationships between the atomic or molecular structure of SE materials and their electrochemical properties. This can enable researchers to identify specific structural features that contribute to enhanced conductivity or stability, aiding in the design of new materials.

Machine learning algorithms, such as support vector machines, random forests, and neural networks, have been employed to correlate material properties with various descriptors, such as chemical composition, crystal structure, and elemental characteristics. These models can then be used to predict the properties of new solid electrolyte materials, guide experimental synthesis and characterization efforts, and accelerate material discovery and optimization. Additionally, the digitalization and ML efforts for SEs are focused on enhancing material characterization techniques, such as X-ray diffraction, Raman spectroscopy, and impedance spectroscopy. ML algorithms can extract valuable insights from these complex datasets, enabling a faster and more accurate analysis and interpretation of the experimental results.

The digitization and ML technologies can provide benefits for fully SSLOBs by improving battery performance, enhancing energy efficiency, and extending their lifespan. However, careful attention should be given to aspects such as reliability, data privacy, and battery safety when implementing these technologies.

#### 4. Recycling of All-Solid-State Lithium Batteries

The materials used in all-solid-state lithium batteries (ASSLBs) can vary depending on the specific design and composition. While some materials, such as lithium, may face availability and scarcity concerns due to increasing demand, efforts are being made to ensure a sustainable supply chain. Exploration of alternative lithium sources, recycling initiatives, and advances in lithium extraction technologies aim to mitigate potential material scarcity issues. Furthermore, ongoing research focuses on developing new battery chemistries that rely on abundant and environmentally friendly materials, reducing reliance on scarce resources.

The recyclability of a piece of technology at the prototype development stage is essential to contributing to a sustainable world. By combining technological development and sustainability, the best technology concept can be achieved in terms of both economic and ecological value. Specific prescriptions and studies for the recycling of ASSLBs are available in the literature. Studies have shown that organic acids, such as citric acid, can

be used for the efficient separation of electrode materials from oxide anodes and electrode materials in ASSLBs [217]. Especially in the case of SPEs, the use of natural polymers for increasing sustainability can be encouraged, since synthetic polymers use hazardous solvents and processing techniques [218]. In the recycling of ceramic solid electrolytes, especially in the recycling of garnet-type electrolytes, strong acids should be used, so environmental pollution should be avoided by choosing the right process [219].

The commercialization of this technology is very important due to the safety and capacity problems experienced in the batteries prepared with liquid electrolytes. ASSLB technology is now a leading competitor in terms of energy density and safety. Babulinca et al. [220] reported that while more than 60 patents were obtained for GPE Li batteries in 2021, this value was only 12 for hybrid electrolytes. In addition, 196 patents were obtained for sulfide solid electrolytes, 42 for garnet solid electrolytes, and 16 patents for perovskite-type solid electrolytes. China, the United States, and Japan are also involved in significant work in the commercialization of solid batteries. They specifically target EV applications with solid inorganic electrolyte technology. As ASSLBs approach commercialization, the importance of recycling these batteries becomes increasingly significant. Developing a clear vision of recycling strategies is essential to prevent the accumulation of used batteries, which could be challenging to recover effectively at their end of life.

When considering SEs recyclability, there are several factors to consider:

1. Material composition. The recyclability of SE materials depends on their chemical composition. Ideally, the materials should be composed of elements that are readily recyclable or can be extracted and reused efficiently.
2. Purity level. The presence of impurities in SE materials can affect their recyclability. Contaminants or unwanted elements may need to be removed or separated during the recycling process.
3. Manufacturing processes. The method used to produce SE materials can impact their recyclability. If the manufacturing process involves techniques that are difficult to reverse or require extensive energy input, it can hinder the material's recyclability.
4. Recycling technologies. Currently, there are various recycling technologies available for different types of materials. The recyclability of SE materials depends on the availability of appropriate recycling technologies that can efficiently recover the material components.
5. Economic feasibility. The economic feasibility of recycling SE materials is an essential consideration. The cost of recycling should be reasonable relative to the cost of producing new materials.
6. Research and development. Continuous research and development efforts are necessary to explore innovative recycling methods for SE materials. This can include the development of new recycling technologies or the improvement of existing ones.

The recyclability of SE materials is a complex issue that involves various factors. As the demand for clean energy technologies grows, it becomes increasingly important to consider the recyclability of the materials used in these devices to minimize their environmental impact.

## 5. Outlook and Perspectives

The lithium–oxygen system is still in its infancy and struggles from a low practical energy density in comparison with the theoretical one. Research in ASSLOBs is rapidly advancing, and it is expected that this technology will play a significant role in the development of sustainable energy storage solutions in the future. In conclusion, while there is still much work to be done, ASSLOBs have the potential to revolutionize the energy storage industry and contribute to a greener future.

**Improved cathode materials:** One way to improve the performance of ASSLOBs is to design more efficient cathode materials, such as metal oxides with a high oxygen reduction potential and low overpotential for oxygen evolution.

Optimized electrolyte design: Another way to enhance the performance of ASSLOBs is to optimize the design of the SE. This can involve incorporating additives or using composite electrolytes to improve ionic conductivity, stability, and selectivity.

Protective coatings: Using protective coatings on the cathode can help prevent oxygen reduction and evolution reactions, reducing capacity fading and improving the cycle life of the battery.

Improved system design: By optimizing the operating conditions of the battery, including temperature and pressure, it is possible to improve the performance of ASSLOBs. Additionally, using advanced control algorithms and modeling techniques can help optimize the charging and discharge processes, leading to improved energy efficiency.

Better understanding of reaction mechanisms: A deeper understanding of the reaction mechanisms taking place in ASSLOBs will provide a foundation for future improvements in this technology. This includes understanding the role of impurities and interfaces in the electrochemical performance of the battery.

In conclusion, there are many avenues for improving ASSLOBs, and ongoing research in this field is expected to lead to significant advancements in the near future.

**Author Contributions:** S.P.: Conceptualization, Validation, Investigation, Writing—Original Draft, Visualization. M.C.: Investigation, Visualization, Writing—Review & Editing. A.G.: Investigation, Validation, Writing—Review & Editing. A.W.M.A.-O.: Investigation, Writing—Review & Editing. T.K.: Writing—Review & Editing, Supervision. All authors have read and agreed to the published version of the manuscript.

**Funding:** This research received no external funding.

**Data Availability Statement:** Not applicable.

**Conflicts of Interest:** The authors declare no conflict of interest.

## References

- Wunderlich, P.; Küpper, J.; Simon, U. Optimizing discharge capacity of graphite nanosheet electrodes for lithium–oxygen batteries. *Batteries* **2020**, *6*, 36. [[CrossRef](#)]
- Ogasawara, T.; Débart, A.; Holzapfel, M.; Novák, P.; Bruce, P.G. Rechargeable Li<sub>2</sub>O<sub>2</sub> electrode for lithium batteries. *J. Am. Chem. Soc.* **2006**, *128*, 1390–1393. [[CrossRef](#)]
- Zheng, H.; Xiao, D.; Li, X.; Liu, Y.; Wu, Y.; Wang, J.; Jiang, K.; Chen, C.; Gu, L.; Wei, X.; et al. New insight in understanding oxygen reduction and evolution in solid-state lithium-oxygen batteries using an in situ environmental scanning electron microscope. *Nano Lett.* **2014**, *14*, 4245–4249. [[CrossRef](#)]
- Manthiram, A.; Yu, X.; Wang, S. Lithium battery chemistries enabled by solid-state electrolytes. *Nat. Rev. Mater.* **2017**, *2*, 16103. [[CrossRef](#)]
- Sun, C.; Liu, J.; Gong, Y.; Wilkinson, D.P.; Zhang, J. Recent advances in all-solid-state rechargeable lithium batteries. *Nano Energy* **2017**, *33*, 363–386. [[CrossRef](#)]
- Xu, R.; Zhang, S.; Wang, X.; Xia, Y.; Xia, X.; Wu, J.; Gu, C.; Tu, J. Recent Developments of All-Solid-State Lithium Secondary Batteries with Sulfide Inorganic Electrolytes. *Chem.-Eur. J.* **2017**, *24*, 6007–6018. [[CrossRef](#)]
- Kim, K.J.; Balaish, M.; Wadaguchi, M.; Kong, L.; Rupp, J.L.M. Solid-State Li–Metal Batteries: Challenges and Horizons of Oxide and Sulfide Solid Electrolytes and Their Interfaces. *Adv. Energy Mater.* **2020**, *11*, 2002689. [[CrossRef](#)]
- Lu, Y.; Zhao, C.; Yuan, H.; Cheng, X.; Huang, J.; Zhang, Q. Critical Current Density in Solid-State Lithium Metal Batteries: Mechanism, Influences, and Strategies. *Adv. Funct. Mater.* **2021**, *31*, 2009925. [[CrossRef](#)]
- Sarkar, S.; Thangadurai, V. Critical Current Densities for High-Performance All-Solid-State Li-Metal Batteries: Fundamentals, Mechanisms, Interfaces, Materials, and Applications. *ACS Energy Lett.* **2022**, *7*, 1492–1527. [[CrossRef](#)]
- Liu, Z.; Huang, J.; Zhang, Y.; Tong, B.; Guo, F.; Wang, J.; Shi, Y.; Wen, R.; Zhou, Z.; Guo, L.; et al. Taming Interfacial Instability in Lithium–Oxygen Batteries: A Polymeric Ionic Liquid Electrolyte Solution. *Adv. Energy Mater.* **2019**, *9*, 1901967. [[CrossRef](#)]
- Wang, X.X.; Chi, X.W.; Li, M.L.; Guan, D.H.; Miao, C.L.; Xu, J.J. An integrated solid-state lithium-oxygen battery with highly stable anionic covalent organic frameworks electrolyte. *Chem* **2022**, *9*, 394–410. [[CrossRef](#)]
- Li, C.; Zhang, S.; Miao, X.; Wang, C.; Zhang, Z.; Wang, R.; Yin, L. Designing Lithium Argyrodite Solid-State Electrolytes for High-Performance All-Solid-State Lithium Batteries. *Batter. Supercaps* **2021**, *5*, e202100288. [[CrossRef](#)]
- Vishnugopi, B.S.; Kazyak, E.; Lewis, J.A.; Nanda, J.; McDowell, M.T.; Dasgupta, N.P.; Mukherjee, P.P. Challenges and Opportunities for Fast Charging of Solid-State Lithium Metal Batteries. *ACS Energy Lett.* **2021**, *6*, 3734–3749. [[CrossRef](#)]
- Wang, J.; Li, Y.; Sun, X. Challenges and opportunities of nanostructured materials for aprotic rechargeable lithium–air batteries. *Nano Energy* **2013**, *2*, 443–467. [[CrossRef](#)]

15. Banerjee, A.; Wang, X.; Fang, C.; Wu, E.A.; Meng, Y.S. Interfaces and Interphases in All-Solid-State Batteries with Inorganic Solid Electrolytes. *Chem. Rev.* **2020**, *120*, 6878–6933. [[CrossRef](#)]
16. Byeon, Y.-W.; Kim, H. Review on Interface and Interphase Issues in Sulfide Solid-State Electrolytes for All-Solid-State Li-Metal Batteries. *Electrochem.* **2021**, *2*, 452–471. [[CrossRef](#)]
17. Ma, L.; Kim, M.S.; Archer, L.A. Stable Artificial Solid Electrolyte Interphases for Lithium Batteries. *Chem. Mater.* **2017**, *29*, 4181–4189. [[CrossRef](#)]
18. Younesi, R.; Hahlin, M.; Roberts, M.; Edström, K. The SEI layer formed on lithium metal in the presence of oxygen: A seldom considered component in the development of the Li-O<sub>2</sub> battery. *J. Power Sources* **2013**, *225*, 40–45. [[CrossRef](#)]
19. Adenusi, H.; Chass, G.A.; Passerini, S.; Tian, K.V.; Chen, G. Lithium Batteries and the Solid Electrolyte Interphase (SEI)—Progress and Outlook. *Adv. Energy Mater.* **2023**, *13*, 2203307. [[CrossRef](#)]
20. Wang, A.; Kadam, S.; Li, H.; Shi, S.; Qi, Y. Review on modeling of the anode solid electrolyte interphase (SEI) for lithium-ion batteries. *npj Comput. Mater.* **2018**, *4*, 15. [[CrossRef](#)]
21. Wang, C.; Adair, K.; Sun, X. All-Solid-State Lithium Metal Batteries with Sulfide Electrolytes: Understanding Interfacial Ion and Electron Transport. *Accounts Mater. Res.* **2021**, *3*, 21–32. [[CrossRef](#)]
22. Kitz, P.G.; Lacey, M.J.; Novák, P.; Berg, E.J. Operando investigation of the solid electrolyte interphase mechanical and transport properties formed from vinylene carbonate and fluoroethylene carbonate. *J. Power Sources* **2020**, *477*, 228567. [[CrossRef](#)]
23. Aurbach, D.; McCloskey, B.D.; Nazar, L.F.; Bruce, P.G. Advances in understanding mechanisms underpinning lithium–air batteries. *Nat. Energy* **2016**, *1*, 16128. [[CrossRef](#)]
24. Park, J.-B.; Lee, S.H.; Jung, H.-G.; Aurbach, D.; Sun, Y.-K. Redox Mediators for Li-O<sub>2</sub>Batteries: Status and Perspectives. *Adv. Mater.* **2017**, *30*, 1704162. [[CrossRef](#)]
25. Jung, J.W.; Cho, S.H.; Nam, J.S.; Kim, I.D. Current and future cathode materials for non-aqueous Li-air (O<sub>2</sub>) battery technology—A focused review. *Energy Storage Mater.* **2019**, *24*, 512–528. [[CrossRef](#)]
26. Zahoor, A.; Ghouri, Z.K.; Hashmi, S.; Raza, F.; Ishtiaque, S.; Nadeem, S.; Ullah, I.; Nahm, K.S. Electrocatalysts for Lithium–Air Batteries: Current Status and Challenges. *ACS Sustain. Chem. Eng.* **2019**, *7*, 14288–14320. [[CrossRef](#)]
27. Liu, Z.; Zhao, Z.; Zhang, W.; Huang, Y.; Liu, Y.; Wu, D.; Wang, L.; Chou, S. Toward high-performance lithium-oxygen batteries with cobalt-based transition metal oxide catalysts: Advanced strategies and mechanical insights. *InfoMat* **2021**, *4*, e12260. [[CrossRef](#)]
28. Chalasani, D.; Lucht, B.L. Reactivity of electrolytes for lithium-oxygen batteries with Li<sub>2</sub>O<sub>2</sub>. *ECS Electrochem. Lett.* **2012**, *1*, A38–A42. [[CrossRef](#)]
29. Yang, T.; Shu, C.; Zheng, R.; Li, M.; Hou, Z.; Hei, P.; Zhang, Q.; Mei, D.; Long, J. Dendrite-Free Solid-State Li-O<sub>2</sub> Batteries Enabled by Organic-Inorganic Interaction Reinforced Gel Polymer Electrolyte. *ACS Sustain. Chem. Eng.* **2019**, *7*, 17362–17371. [[CrossRef](#)]
30. Cao, D.; Sun, X.; Li, Q.; Natan, A.; Xiang, P.; Zhu, H. Lithium Dendrite in All-Solid-State Batteries: Growth Mechanisms, Suppression Strategies, and Characterizations. *Matter* **2020**, *3*, 57–94. [[CrossRef](#)]
31. Sastre, J.; Futscher, M.H.; Pompizi, L.; Aribia, A.; Priebe, A.; Overbeck, J.; Stiefel, M.; Tiwari, A.N.; Romanyuk, Y.E. Blocking lithium dendrite growth in solid-state batteries with an ultrathin amorphous Li-La-Zr-O solid electrolyte. *Commun. Mater.* **2021**, *2*, 76. [[CrossRef](#)]
32. Xin, X.; Ito, K.; Dutta, A.; Kubo, Y. Dendrite-Free Epitaxial Growth of Lithium Metal during Charging in Li-O<sub>2</sub> Batteries. *Angew. Chem. Int. Ed.* **2018**, *57*, 13206–13210. [[CrossRef](#)]
33. Hou, G.; Ma, X.; Sun, Q.; Ai, Q.; Xu, X.; Chen, L.; Li, D.; Chen, J.; Zhong, H.; Li, Y.; et al. Lithium Dendrite Suppression and Enhanced Interfacial Compatibility Enabled by an Ex Situ SEI on Li Anode for LAGP-Based All-Solid-State Batteries. *ACS Appl. Mater. Interfaces* **2018**, *10*, 18610–18618. [[CrossRef](#)]
34. Kang, J.-H.; Park, J.; Na, M.; Choi, R.H.; Byon, H.R. Low-Temperature CO<sub>2</sub>-Assisted Lithium–Oxygen Batteries for Improved Stability of Peroxodicarbonate and Excellent Cyclability. *ACS Energy Lett.* **2022**, *7*, 4248–4257. [[CrossRef](#)]
35. Liu, H.; Cheng, X.; Yan, C.; Li, Z.; Zhao, C.; Xiang, R.; Yuan, H.; Huang, J.; Kuzmina, E.; Karaseva, E.; et al. A perspective on energy chemistry of low-temperature lithium metal batteries. *iEnergy* **2022**, *1*, 72–81. [[CrossRef](#)]
36. Zhang, N.; Deng, T.; Zhang, S.; Wang, C.; Chen, L.; Wang, C.; Fan, X. Critical Review on Low-Temperature Li-Ion/Metal Batteries. *Adv. Mater.* **2022**, *34*, 2107899. [[CrossRef](#)]
37. Hu, A.; Li, F.; Chen, W.; Lei, T.; Li, Y.; Fan, Y.; He, M.; Wang, F.; Zhou, M.; Hu, Y.; et al. Ion Transport Kinetics in Low-Temperature Lithium Metal Batteries. *Adv. Energy Mater.* **2022**, *12*, 2202432. [[CrossRef](#)]
38. Luo, D.; Li, M.; Zheng, Y.; Ma, Q.; Gao, R.; Zhang, Z.; Dou, H.; Wen, G.; Shui, L.; Yu, A.; et al. Electrolyte Design for Lithium Metal Anode-Based Batteries Toward Extreme Temperature Application. *Adv. Sci.* **2021**, *8*, 2101051. [[CrossRef](#)] [[PubMed](#)]
39. Wang, S.; Song, H.; Song, X.; Zhu, T.; Ye, Y.; Chen, J.; Yu, L.; Xu, J.; Chen, K. An extra-wide temperature all-solid-state lithium-metal battery operating from –73 °C to 120 °C. *Energy Storage Mater.* **2021**, *39*, 139–145. [[CrossRef](#)]
40. Kitaura, H.; Zhou, H. All-solid-state lithium-oxygen battery with high safety in wide ambient temperature range. *Sci. Rep.* **2015**, *5*, 13271. [[CrossRef](#)]
41. Chi, X.; Li, M.; Di, J.; Bai, P.; Song, L.; Wang, X.; Li, F.; Liang, S.; Xu, J.; Yu, J. A highly stable and flexible zeolite electrolyte solid-state Li–air battery. *Nature* **2021**, *592*, 551–557. [[CrossRef](#)] [[PubMed](#)]
42. Wang, H.-F.; Wang, X.-X.; Li, F.; Xu, J.-J. Fundamental Understanding and Construction of Solid-State Li–Air Batteries. *Small Sci.* **2022**, *2*, 2200005. [[CrossRef](#)]

43. Yang, C.-S.; Gao, K.-N.; Zhang, X.-P.; Sun, Z.; Zhang, T. Rechargeable solid-state Li-air batteries: A status report. *Rare Met.* **2018**, *37*, 459–472. [[CrossRef](#)]
44. Liu, Y.; Zhao, Y.; Lu, W.; Sun, L.; Lin, L.; Zheng, M.; Sun, X.; Xie, H. PEO based polymer in plastic crystal electrolytes for room temperature high-voltage lithium metal batteries. *Nano Energy* **2021**, *88*, 106205. [[CrossRef](#)]
45. Wu, Y.; Li, Y.; Wang, Y.; Liu, Q.; Chen, Q.; Chen, M. Advances and prospects of PVDF based polymer electrolytes. *J. Energy Chem.* **2021**, *64*, 62–84. [[CrossRef](#)]
46. Tang, B.; Zhou, Q.; Du, X.; Zhang, J.; Zhang, H.; Zou, Z.; Zhou, X.; Cui, G. Poly(maleic anhydride) copolymers-based polymer electrolytes enlighten highly safe and high-energy-density lithium metal batteries: Advances and prospects. *Nano Sel.* **2020**, *1*, 59–78. [[CrossRef](#)]
47. Yi, J.; Guo, S.; He, P.; Zhou, H. Status and prospects of polymer electrolytes for solid-state Li-O<sub>2</sub> (air) batteries. *Energy Environ. Sci.* **2017**, *10*, 860–884. [[CrossRef](#)]
48. Buannic, L.; Naviroj, M.; Miller, S.M.; Zagorski, J.; Faber, K.T.; Llordés, A. Dense freeze-cast Li<sub>7</sub>La<sub>3</sub>Zr<sub>2</sub>O<sub>12</sub> solid electrolytes with oriented open porosity and contiguous ceramic scaffold. *J. Am. Ceram. Soc.* **2018**, *102*, 1021–1029. [[CrossRef](#)]
49. Wang, M.; Wu, Y.; Qiu, M.; Li, X.; Li, C.; Li, R.; He, J.; Lin, G.; Qian, Q.; Wen, Z.; et al. Research progress in electrospinning engineering for all-solid-state electrolytes of lithium metal batteries. *J. Energy Chem.* **2021**, *61*, 253–268. [[CrossRef](#)]
50. McOwen, D.W.; Xu, S.; Gong, Y.; Wen, Y.; Godbey, G.L.; Gritton, J.E.; Hamann, T.R.; Dai, J.; Hitz, G.T.; Hu, L.; et al. 3D-Printing Electrolytes for Solid-State Batteries. *Adv. Mater.* **2018**, *30*, e1707132. [[CrossRef](#)]
51. Chen, A.; Qu, C.; Shi, Y.; Shi, F. Manufacturing Strategies for Solid Electrolyte in Batteries. *Front. Energy Res.* **2020**, *8*, 571440. [[CrossRef](#)]
52. Boaretto, N.; Garbayo, I.; Valiyaveettil-SobhanRaj, S.; Quintela, A.; Li, C.; Casas-Cabanas, M.; Aguesse, F. Lithium solid-state batteries: State-of-the-art and challenges for materials, interfaces and processing. *J. Power Sources* **2021**, *502*, 229919. [[CrossRef](#)]
53. Zaman, W.; Hatzell, K.B. Processing and manufacturing of next generation lithium-based all solid-state batteries. *Curr. Opin. Solid State Mater. Sci.* **2022**, *26*, 101003. [[CrossRef](#)]
54. Ren, Y.; Chen, K.; Chen, R.; Liu, T.; Zhang, Y.; Nan, C.W. Oxide Electrolytes for Lithium Batteries. *J. Am. Ceram. Soc.* **2015**, *98*, 3603–3623. [[CrossRef](#)]
55. Ma, Q.; Xu, Q.; Tsai, C.L.; Tietz, F.; Guillot, O. A Novel Sol-Gel Method for Large-Scale Production of Nanopowders: Preparation of Li<sub>1.5</sub>Al<sub>0.5</sub>Ti<sub>1.5</sub>(PO<sub>4</sub>)<sub>3</sub> as an Example. *J. Am. Ceram. Soc.* **2015**, *99*, 410–414. [[CrossRef](#)]
56. Kang, I.; Kang, J. Low-cost iron-based electrocatalysts for high-performance Li-O<sub>2</sub> batteries. *Results Mater.* **2023**, *17*, 100351. [[CrossRef](#)]
57. Zhao, Z.; Pan, L.; Li, Y.; Wang, J.; Luo, Z.; Chen, W.; Liu, Z.; He, H. Aluminum silicate fiber membrane: A cost-effective substitute for fiber glass separator in Li-O<sub>2</sub> battery. *Mater. Today Energy* **2020**, *17*, 100485. [[CrossRef](#)]
58. Schnell, J.; Günther, T.; Knoche, T.; Vieider, C.; Köhler, L.; Just, A.; Keller, M.; Passerini, S.; Reinhart, G. All-solid-state lithium-ion and lithium metal batteries—Paving the way to large-scale production. *J. Power Sources* **2018**, *382*, 160–175. [[CrossRef](#)]
59. Zhao, H.; Ma, Y.; Qi, H.; Xiao, Z.; Lin, H.; Liu, J.; Guo, Z.; Wang, L.; Feng, S. A dendrite-free and stable anode for high-performance Li-O<sub>2</sub> batteries by prestoring Li in reduced graphene oxide coated three-dimensional nickel foam. *Chem. Commun.* **2020**, *56*, 7645–7648. [[CrossRef](#)]
60. Huang, G.; Wang, J.; Zhang, X. Electrode Protection in High-Efficiency Li-O<sub>2</sub> Batteries. *ACS Central Sci.* **2020**, *6*, 2136–2148. [[CrossRef](#)]
61. Yu, Y.; Liu, Y.; Xie, J. Building Better Li Metal Anodes in Liquid Electrolyte: Challenges and Progress. *ACS Appl. Mater. Interfaces* **2020**, *13*, 18–33. [[CrossRef](#)]
62. Li, J.; Kong, Z.; Liu, X.; Zheng, B.; Fan, Q.H.; Garratt, E.; Schuelke, T.; Wang, K.; Xu, H.; Jin, H. Strategies to anode protection in lithium metal battery: A review. *InfoMat* **2021**, *3*, 1333–1363. [[CrossRef](#)]
63. Guo, Z.; Li, J.; Xia, Y.; Chen, C.; Wang, F.; Tamirat, A.G.; Wang, Y.; Xia, Y.; Wang, L.; Feng, S. A flexible polymer-based Li-air battery using a reduced graphene oxide/Li composite anode. *J. Mater. Chem. A* **2018**, *6*, 6022–6032. [[CrossRef](#)]
64. Deng, H.; Qiu, F.; Li, X.; Qin, H.; Zhao, S.; He, P.; Zhou, H. A Li-ion oxygen battery with Li-Si alloy anode prepared by a mechanical method. *Electrochim. Commun.* **2017**, *78*, 11–15. [[CrossRef](#)]
65. Guo, Z.; Dong, X.; Wang, Y.; Xia, Y. Correction: A lithium air battery with a lithiated Al–carbon anode. *Chem. Commun.* **2021**, *57*, 3724. [[CrossRef](#)]
66. Wang, H.; Wang, X.; Li, M.; Zheng, L.; Guan, D.; Huang, X.; Xu, J.; Yu, J. Porous Materials Applied in Nonaqueous Li-O<sub>2</sub> Batteries: Status and Perspectives. *Adv. Mater.* **2020**, *32*, 2002559. [[CrossRef](#)]
67. Jeong, M.G.; Kwak, W.J.; Kim, J.Y.; Lee, J.K.; Sun, Y.K.; Jung, H.G. Uniformly distributed reaction by 3D host-lithium composite anode for high rate capability and reversibility of Li-O<sub>2</sub> batteries. *Chem. Eng. J.* **2021**, *427*, 130914. [[CrossRef](#)]
68. Ma, Y.; Wei, L.; Gu, Y.; Hu, J.; Chen, Y.; Qi, P.; Zhao, X.; Peng, Y.; Deng, Z.; Liu, Z. High-Performance Li-O<sub>2</sub> Batteries Based on All-Graphene Backbone. *Adv. Funct. Mater.* **2020**, *30*, 2007218. [[CrossRef](#)]
69. Luo, Z.; Zhu, G.; Yin, L.; Li, F.; Bin Xu, B.; Dala, L.; Liu, X.; Luo, K. A Facile Surface Preservation Strategy for the Lithium Anode for High-Performance Li-O<sub>2</sub> Batteries. *ACS Appl. Mater. Interfaces* **2020**, *12*, 27316–27326. [[CrossRef](#)]
70. Xia, Q.; Zan, F.; Zhang, Q.; Liu, W.; Li, Q.; He, Y.; Hua, J.; Liu, J.; Xu, J.; Wang, J.; et al. All-Solid-State Thin Film Lithium/Lithium-Ion Microbatteries for Powering the Internet of Things. *Adv. Mater.* **2022**, *35*, 2200538. [[CrossRef](#)]

71. Tian, Y.; An, Y.; Wei, C.; Jiang, H.; Xiong, S.; Feng, J.; Qian, Y. Recently advances and perspectives of anode-free rechargeable batteries. *Nano Energy* **2020**, *78*, 105344. [[CrossRef](#)]
72. Hsueh, T.H.; Wang, M.-C.; Liu, S.-E.; Wu, B.-H.; Li, Y.-C.; Tsai, D.-G.; Chang, S.-M.; Shiue, A.; Chin, K.-Y. Sputtered silver on the current collector for anode-less NMC111 gel polymer electrolyte lithium batteries. *Electrochim. Commun.* **2023**, *150*, 107478. [[CrossRef](#)]
73. Nikodimos, Y.; Su, W.-N.; Shitaw, K.N.; Jiang, S.-K.; Abrha, L.H.; Weret, M.A.; Merso, S.K.; Hagos, T.M.; Huang, C.-J.; Lakshmanan, K.; et al. Multifunctional Electrospun PVDF-HFP Gel Polymer Electrolyte Membrane Suppresses Dendrite Growth in Anode-Free Li Metal Battery. *Energy Storage Mater.* **2023**, *61*, 102861. [[CrossRef](#)]
74. Hasegawa, S.; Imanishi, N.; Zhang, T.; Xie, J.; Hirano, A.; Takeda, Y.; Yamamoto, O. Study on lithium/air secondary batteries-Stability of NASICON-type lithium ion conducting glass-ceramics with water. *J. Power Sources* **2009**, *189*, 371–377. [[CrossRef](#)]
75. Bai, F.; Kakimoto, K.; Shang, X.; Mori, D.; Taminato, S.; Matsumoto, M.; Takeda, Y.; Yamamoto, O.; Izumi, H.; Minami, H.; et al. Water-Stable High Lithium-Ion Conducting Solid Electrolyte of  $\text{Li}_{1.4}\text{Al}_{0.4}\text{Ge}_{0.2}\text{Ti}_{1.4}(\text{PO}_4)_3\text{-LiCl}$  for Aqueous Lithium-Air Batteries. *Front. Energy Res.* **2020**, *8*, 187. [[CrossRef](#)]
76. Hartmann, P.; Leichtweiss, T.; Busche, M.R.; Schneider, M.; Reich, M.; Sann, J.; Adelhelm, P.; Janek, J. Degradation of NASICON-Type Materials in Contact with Lithium Metal: Formation of Mixed Conducting Interphases (MCI) on Solid Electrolytes. *J. Phys. Chem. C* **2013**, *117*, 21064–21074. [[CrossRef](#)]
77. Lewis, J.A.; Cortes, F.J.Q.; Boebinger, M.G.; Tippens, J.; Marchese, T.S.; Kondekar, N.P.; Liu, X.; Chi, M.; McDowell, M.T. Interphase Morphology between a Solid-State Electrolyte and Lithium Controls Cell Failure. *ACS Energy Lett.* **2019**, *4*, 591–599. [[CrossRef](#)]
78. Li, Y.; Wang, H. Composite Solid Electrolytes with NASICON-Type LATP and PVdF-HFP for Solid-State Lithium Batteries. *Ind. Eng. Chem. Res.* **2021**, *60*, 1494–1500. [[CrossRef](#)]
79. Yow, Z.F.; Oh, Y.L.; Gu, W.; Rao, R.P.; Adams, S. Effect of  $\text{Li}^+/\text{H}^+$  exchange in water treated Ta-doped  $\text{Li}_7\text{La}_3\text{Zr}_2\text{O}_{12}$ . *Solid State Ion.* **2016**, *292*, 122–129. [[CrossRef](#)]
80. Zeng, X.; Martinolich, A.J.; See, K.A.; Faber, K.T. Dense garnet-type electrolyte with coarse grains for improved air stability and ionic conductivity. *J. Energy Storage* **2019**, *27*, 101128. [[CrossRef](#)]
81. Huang, B.; Xu, B.; Zhang, J.; Li, Z.; Huang, Z.; Li, Y.; Wang, C.-A. Li-ion conductivity and stability of hot-pressed  $\text{LiTa}_2\text{PO}_8$  solid electrolyte for all-solid-state batteries. *J. Mater. Sci.* **2020**, *56*, 2425–2434. [[CrossRef](#)]
82. Liu, X.-Z.; Ding, L.; Liu, Y.-Z.; Xiong, L.-P.; Chen, J.; Luo, X.-L. Room-temperature ionic conductivity of Ba, Y, Al co-doped  $\text{Li}_7\text{La}_3\text{Zr}_2\text{O}_{12}$  solid electrolyte after sintering. *Rare Met.* **2020**, *40*, 2301–2306. [[CrossRef](#)]
83. Wang, C.; Fu, K.; Kammampata, S.P.; McOwen, D.W.; Samson, A.J.; Zhang, L.; Hitz, G.T.; Nolan, A.M.; Wachsman, E.D.; Mo, Y.; et al. Garnet-Type Solid-State Electrolytes: Materials, Interfaces, and Batteries. *Chem. Rev.* **2020**, *120*, 4257–4300. [[CrossRef](#)]
84. Inada, R.; Kimura, K.; Kusakabe, K.; Tojo, T.; Sakurai, Y. Synthesis and lithium-ion conductivity for perovskite-type  $\text{Li}_{3/8}\text{Sr}_{7/16}\text{Ta}_{3/4}\text{Zr}_{1/4}\text{O}_3$  solid electrolyte by powder-bed sintering. *Solid State Ion.* **2014**, *261*, 95–99. [[CrossRef](#)]
85. Li, Y.; Xu, H.; Chien, P.; Wu, N.; Xin, S.; Xue, L.; Park, K.; Hu, Y.; Goodenough, J.B. A Perovskite Electrolyte That Is Stable in Moist Air for Lithium-Ion Batteries. *Angew. Chem. Int. Ed.* **2018**, *57*, 8587–8591. [[CrossRef](#)]
86. Ma, S.B.; Kwon, H.J.; Kim, M.; Bak, S.; Lee, H.; Ehrlich, S.N.; Cho, J.; Im, D.; Seo, D. Mixed Ionic–Electronic Conductor of Perovskite  $\text{Li}_x\text{La}_y\text{Mo}_3-\delta$  toward Carbon-Free Cathode for Reversible Lithium–Air Batteries. *Adv. Energy Mater.* **2020**, *10*, 2001767. [[CrossRef](#)]
87. Lim, C.; Kim, C.; Gwon, O.; Jeong, H.Y.; Song, H.-K.; Ju, Y.-W.; Shin, J.; Kim, G. Nano-perovskite oxide prepared via inverse microemulsion mediated synthesis for catalyst of lithium-air batteries. *Electrochim. Acta* **2018**, *275*, 248–255. [[CrossRef](#)]
88. Zhou, Y.; Gu, Q.; Li, Y.; Tao, L.; Tan, H.; Yin, K.; Zhou, J.; Guo, S. Cesium Lead Bromide Perovskite-Based Lithium-Oxygen Batteries. *Nano Lett.* **2021**, *21*, 4861–4867. [[CrossRef](#)]
89. Sahu, G.; Lin, Z.; Li, J.; Liu, Z.; Dudney, N.; Liang, C. Air-stable, high-conduction solid electrolytes of arsenic-substituted  $\text{Li}_4\text{SnS}_4$ . *Energy Environ. Sci.* **2013**, *7*, 1053–1058. [[CrossRef](#)]
90. Wang, Y.; Lü, X.; Zheng, C.; Liu, X.; Chen, Z.; Yang, W.; Lin, J.; Huang, F. Chemistry Design Towards a Stable Sulfide-Based Superionic Conductor  $\text{Li}_4\text{Cu}_8\text{Ge}_3\text{S}_{12}$ . *Angew. Chem. Int. Ed.* **2019**, *58*, 7673–7677. [[CrossRef](#)]
91. Ohtomo, T.; Hayashi, A.; Tatsumisago, M.; Kawamoto, K. Characteristics of the  $\text{Li}_2\text{O}-\text{Li}_2\text{S}-\text{P}_2\text{S}_5$  glasses synthesized by the two-step mechanical milling. *J. Non-Cryst. Solids* **2013**, *364*, 57–61. [[CrossRef](#)]
92. Otoyama, M.; Kuratani, K.; Kobayashi, H. A systematic study on structure, ionic conductivity, and air-stability of  $x\text{Li}_4\text{SnS}_4\cdot(1-x)\text{Li}_3\text{PS}_4$  solid electrolytes. *Ceram. Int.* **2021**, *47*, 28377–28383. [[CrossRef](#)]
93. Zhang, Q.; Cao, D.; Ma, Y.; Natan, A.; Aurora, P.; Zhu, H. Sulfide-Based Solid-State Electrolytes: Synthesis, Stability, and Potential for All-Solid-State Batteries. *Adv. Mater.* **2019**, *31*, e1901131. [[CrossRef](#)] [[PubMed](#)]
94. Hangofer, I.; Redhammer, G.; Rohde, S.; Hanzu, I.; Senyshyn, A.; Wilkening, H.M.R.; Rettenwander, D. Untangling the Structure and Dynamics of Lithium-Rich Anti-Perovskites Envisaged as Solid Electrolytes for Batteries. *Chem. Mater.* **2018**, *30*, 8134–8144. [[CrossRef](#)]
95. Emly, A.; Kioupakis, E.; Van der Ven, A. Phase Stability and Transport Mechanisms in Antiperovskite  $\text{Li}_3\text{OCl}$  and  $\text{Li}_3\text{OBr}$  Superionic Conductors. *Chem. Mater.* **2013**, *25*, 4663–4670. [[CrossRef](#)]
96. Mohamed, M.A.A.; Gorbunov, M.V.; Valldor, M.; Hampel, S.; Gräßler, N.; Mikhailova, D. Tuning the electrochemical properties by anionic substitution of Li-rich antiperovskite  $(\text{Li}_2\text{Fe})\text{S}_{1-x}\text{Se}_x\text{O}$  cathodes for Li-ion batteries. *J. Mater. Chem. A* **2021**, *9*, 23095–23105. [[CrossRef](#)]

97. Li, S.; Zhu, J.; Wang, Y.; Howard, J.W.; Lü, X.; Li, Y.; Kumar, R.S.; Wang, L.; Daemen, L.L.; Zhao, Y. Reaction mechanism studies towards effective fabrication of lithium-rich anti-perovskites  $\text{Li}_3\text{OX}$  ( $X = \text{Cl}, \text{Br}$ ). *Solid State Ion.* **2016**, *284*, 14–19. [CrossRef]
98. Senevirathne, K.; Day, C.S.; Gross, M.D.; Lachgar, A.; Holzwarth, N. A new crystalline LiPON electrolyte: Synthesis, properties, and electronic structure. *Solid State Ion.* **2013**, *233*, 95–101. [CrossRef]
99. Jadhav, H.S.; Kalubarme, R.S.; Jadhav, A.H.; Gil Seo, J. Highly stable bilayer of LiPON and  $\text{B}_2\text{O}_3$  added  $\text{Li}_{1.5}\text{Al}_{0.5}\text{Ge}_{1.5}(\text{PO}_4)$  solid electrolytes for non-aqueous rechargeable  $\text{Li}-\text{O}_2$  batteries. *Electrochim. Acta* **2016**, *199*, 126–132. [CrossRef]
100. Goodenough, J.B.; Hong, H.Y.-P.; Kafalas, J.A. Fast  $\text{Na}^+$ -ion transport in skeleton structures. *Mater. Res. Bull.* **1976**, *11*, 203–220. [CrossRef]
101. Thangadurai, V.; Weppner, W. Recent progress in solid oxide and lithium ion conducting electrolytes research. *Ionics* **2006**, *12*, 81–92. [CrossRef]
102. Steinle, D.; Wu, F.; Kim, G.-T.; Passerini, S.; Bresser, D. PEO-based Interlayers for LAGP-type Solid-State Lithium-Metal Batteries. In *Electrochemical Society Meeting Abstracts* **242**; No. 4; The Electrochemical Society, Inc.: Atlanta, GA, USA, 2022. [CrossRef]
103. Dussart, T.; Stevens, P.; Toussaint, G.; Laberty-Robert, C. Study of Solid State Lithium Batteries with a Ceramic Electrolyte. In *Electrochemical Society Meeting Abstracts* **237**; No. 2; The Electrochemical Society, Inc.: Montréal, QC, Canada, 2022. [CrossRef]
104. Thangadurai, V.; Narayanan, S.; Pinzar, D. Garnet-type solid-state fast Li ion conductors for Li batteries: Critical review. *Chem. Soc. Rev.* **2014**, *43*, 4714–4727. [CrossRef]
105. Thangadurai, V.; Kaack, H.; Weppner, W.J.F. Novel Fast Lithium Ion Conduction in Garnet-Type  $\text{Li}_5\text{La}_3\text{M}_2\text{O}_{12}$  ( $\text{M} = \text{Nb}, \text{Ta}$ ). *J. Am. Ceram. Soc.* **2003**, *86*, 437–440. [CrossRef]
106. Murugan, R.; Thangadurai, V.; Weppner, W. Fast lithium ion conduction in garnet-type  $\text{Li}_7\text{La}_3\text{Zr}_2\text{O}_{12}$ . *Angew. Chem. Int. Ed.* **2007**, *46*, 7778–7781. [CrossRef]
107. Qin, S.; Zhu, X.; Jiang, Y.; Ling, M.; Hu, Z.; Zhu, J. Growth of self-textured  $\text{Ga}^{3+}$ -substituted  $\text{Li}_7\text{La}_3\text{Zr}_2\text{O}_{12}$  ceramics by solid state reaction and their significant enhancement in ionic conductivity. *Appl. Phys. Lett.* **2018**, *112*, 113901. [CrossRef]
108. Meesala, Y.; Jena, A.; Chang, H.; Liu, R.-S. Recent Advancements in Li-Ion Conductors for All-Solid-State Li-Ion Batteries. *ACS Energy Lett.* **2017**, *2*, 2734–2751. [CrossRef]
109. Kobi, S.; Amardeep; Vyas, A.; Bhargava, P.; Mukhopadhyay, A. Al and Mg Co-Doping Towards Development of Air-Stable and Li-Ion Conducting Li-La-Zirconate Based Solid Electrolyte Exhibiting Low Electrode/Electrolyte Interfacial Resistance. *J. Electrochem. Soc.* **2020**, *167*, 120519. [CrossRef]
110. Abrha, L.H.; Hagos, T.T.; Nikodimos, Y.; Bezabh, H.K.; Berhe, G.B.; Hagos, T.M.; Huang, C.-J.; Tegegne, W.A.; Jiang, S.-K.; Weldeyohannes, H.H.; et al. Dual-Doped Cubic Garnet Solid Electrolytes with Superior Air Stability. *ACS Appl. Mater. Interfaces* **2020**, *12*, 25709–25717. [CrossRef]
111. Jin, Y.; McGinn, P.J.  $\text{Li}_7\text{La}_3\text{Zr}_2\text{O}_{12}$  electrolyte stability in air and fabrication of a  $\text{Li}/\text{Li}_7\text{La}_3\text{Zr}_2\text{O}_{12}/\text{Cu}_{0.1}\text{V}_2\text{O}_5$  solid-state battery. *J. Power Sources* **2013**, *239*, 326–331. [CrossRef]
112. Jia, M.; Bi, Z.; Shi, C.; Zhao, N.; Guo, X. Air-stable dopamine-treated garnet ceramic particles for high-performance composite electrolytes. *J. Power Sources* **2020**, *486*, 229363. [CrossRef]
113. Duan, H.; Chen, W.; Fan, M.; Wang, W.; Yu, L.; Tan, S.; Chen, X.; Zhang, Q.; Xin, S.; Wan, L.; et al. Building an Air Stable and Lithium Deposition Regulable Garnet Interface from Moderate-Temperature Conversion Chemistry. *Angew. Chem. Int. Ed.* **2020**, *59*, 12069–12075. [CrossRef]
114. Li, R.; Liao, K.; Zhou, W.; Li, X.; Meng, D.; Cai, R.; Shao, Z. Realizing fourfold enhancement in conductivity of perovskite  $\text{Li}_{0.33}\text{La}_{0.557}\text{TiO}_3$  electrolyte membrane via a Sr and Ta co-doping strategy. *J. Membr. Sci.* **2019**, *582*, 194–202. [CrossRef]
115. Le, H.T.T.; Ngo, D.T.; Didwal, P.N.; Fisher, J.G.; Park, C.-N.; Kim, I.-D.; Park, C.-J. Highly efficient and stable solid-state  $\text{Li}-\text{O}_2$  batteries using a perovskite solid electrolyte. *J. Mater. Chem. A* **2019**, *7*, 3150–3160. [CrossRef]
116. Xu, H.; Chien, P.-H.; Shi, J.; Li, Y.; Wu, N.; Liu, Y.; Hu, Y.-Y.; Goodenough, J.B. High-performance all-solid-state batteries enabled by salt bonding to perovskite in poly(ethylene oxide). *Proc. Natl. Acad. Sci. USA* **2019**, *116*, 18815–18821. [CrossRef]
117. Dawson, J.A.; Famprakis, T.; Johnston, K.E. Anti-perovskites for solid-state batteries: Recent developments, current challenges and future prospects. *J. Mater. Chem. A* **2021**, *9*, 18746–18772. [CrossRef]
118. Dixit, M.; Muralidharan, N.; Bisht, A.; Jafta, C.J.; Nelson, C.T.; Amin, R.; Essehli, R.; Balasubramanian, M.; Belharouak, I. Tailoring of the Anti-Perovskite Solid Electrolytes at the Grain-Scale. *ACS Energy Lett.* **2023**, *8*, 2356–2364. [CrossRef]
119. Ye, Y.; Deng, Z.; Gao, L.; Niu, K.; Zhao, R.; Bian, J.; Li, S.; Lin, H.; Zhu, J.; Zhao, Y. Lithium-Rich Anti-perovskite  $\text{Li}_2\text{OHBr}$ -Based Polymer Electrolytes Enabling an Improved Interfacial Stability with a Three-Dimensional-Structured Lithium Metal Anode in All-Solid-State Batteries. *ACS Appl. Mater. Interfaces* **2021**, *13*, 28108–28117. [CrossRef]
120. Xia, W.; Zhao, Y.; Zhao, F.; Adair, K.; Zhao, R.; Li, S.; Zou, R.; Zhao, Y.; Sun, X. Antiperovskite Electrolytes for Solid-State Batteries. *Chem. Rev.* **2022**, *122*, 3763–3819. [CrossRef]
121. Deng, Z.; Ni, D.; Chen, D.; Bian, Y.; Li, S.; Wang, Z.; Zhao, Y. Anti-perovskite materials for energy storage batteries. *InfoMat* **2021**, *4*, e12252. [CrossRef]
122. Yu, P.; Ye, Y.; Zhu, J.; Xia, W.; Zhao, Y. Optimized Interfaces in Anti-Perovskite Electrolyte-Based Solid-State Lithium Metal Batteries for Enhanced Performance. *Front. Chem.* **2021**, *9*, 786956. [CrossRef]
123. Fang, H.; Jena, P. Li-rich antiperovskite superionic conductors based on cluster ions. *Proc. Natl. Acad. Sci. USA* **2017**, *114*, 11046–11051. [CrossRef] [PubMed]

124. Zheng, F.; Kotobuki, M.; Song, S.; Lai, M.O.; Lu, L. Review on solid electrolytes for all-solid-state lithium-ion batteries. *J. Power Sources* **2018**, *389*, 198–213. [[CrossRef](#)]
125. Li, M.; Chi, X.; Yu, J. Zeolite-Based Electrolytes: A Promising Choice for Solid-State Batteries. *PRX Energy* **2022**, *1*, 031001. [[CrossRef](#)]
126. Ding, Z.; Tang, Q.; Liu, Y.; Yao, P.; Liu, C.; Liu, X.; Wu, J.; Lavorgna, M. Integrate multifunctional ionic sieve lithiated X zeolite-ionic liquid electrolyte for solid-state lithium metal batteries with ultralong lifespan. *Chem. Eng. J.* **2021**, *433*, 133522. [[CrossRef](#)]
127. Yang, C.; Wang, Y.; Alfutimie, A. Comparison of Nature and Synthetic Zeolite for Waste Battery Electrolyte Treatment in Fixed-Bed Adsorption Column. *Energies* **2022**, *15*, 347. [[CrossRef](#)]
128. Ding, Z.; Tang, Q.; Zhang, Q.; Yao, P.; Liu, X.; Wu, J. A flexible solid polymer electrolyte enabled with lithiated zeolite for high performance lithium battery. *Nano Res.* **2023**, *1*–10. [[CrossRef](#)]
129. Chen, X.; Guan, Z.; Chu, F.; Xue, Z.; Wu, F.; Yu, Y. Air-stable inorganic solid-state electrolytes for high energy density lithium batteries: Challenges, strategies, and prospects. *InfoMat* **2021**, *4*, e12248. [[CrossRef](#)]
130. Barbosa, J.C.; Gonçalves, R.; Costa, C.M.; Bermudez, V.d.Z.; Fidalgo-Marijuan, A.; Zhang, Q.; Lanceros-Méndez, S. Metal-organic frameworks and zeolite materials as active fillers for lithium-ion battery solid polymer electrolytes. *Mater. Adv.* **2021**, *2*, 3790–3805. [[CrossRef](#)]
131. Le, H.T.T.; Ngo, D.T.; Kim, Y.J.; Park, C.N.; Park, C.J. A perovskite-structured aluminium-substituted lithium lanthanum titanate as a potential artificial solid-electrolyte interface for aqueous rechargeable lithium-metal-based batteries. *Electrochim. Acta* **2017**, *248*, 232–242. [[CrossRef](#)]
132. Khan, T.T.; Park, C.-J. Solid-State Li-O<sub>2</sub> Battery Using a Perovskite Type Solid Electrolyte with an Improved Interfacial Property. In *Electrochemical Society Meeting Abstracts* 235; No. 2; The Electrochemical Society, Inc.: Dallas, TX, USA, 2019. [[CrossRef](#)]
133. Li, B.; Liu, Y.; Zhang, X.; He, P.; Zhou, H. Hybrid polymer electrolyte for Li-O<sub>2</sub> batteries. *Green Energy Environ.* **2018**, *4*, 3–19. [[CrossRef](#)]
134. Yi, J.; Zhou, H. A Unique Hybrid Quasi-Solid-State Electrolyte for Li-O<sub>2</sub> Batteries with Improved Cycle Life and Safety. *Chem-suschem* **2016**, *9*, 2391–2396. [[CrossRef](#)] [[PubMed](#)]
135. Sashmitha, K.; Rani, M.U. A comprehensive review of polymer electrolyte for lithium-ion battery. *Polym. Bull.* **2022**, *80*, 89–135. [[CrossRef](#)]
136. Tsutsumi, H.; Matsuo, A.; Takase, K.; Doi, S.; Hisanaga, A.; Onimura, K.; Oishi, T. Conductivity enhancement of polyacrylonitrile-based electrolytes by addition of cascade nitrile compounds. *J. Power Sources* **2000**, *90*, 33–38. [[CrossRef](#)]
137. Li, S.; Ren, W.; Huang, Y.; Zhou, Q.; Luo, C.; Li, Z.; Li, X.; Wang, M.; Cao, H. Building more secure LMBs with gel polymer electrolytes based on dual matrices of PAN and HPMC by improving compatibility with anode and tuning lithium ion transference. *Electrochim. Acta* **2021**, *391*, 138950. [[CrossRef](#)]
138. Huq, R.; Koksbang, R.; Tonder, P.; Farrington, G.C. Effect of plasticizers on the properties of new ambient temperature polymer electrolyte. *Electrochim. Acta* **1992**, *37*, 1681–1684. [[CrossRef](#)]
139. Abraham, K.M.; Alamgir, M. Li<sup>+</sup>-Conductive Solid Polymer Electrolytes with Liquid-Like Conductivity. *J. Electrochem. Soc.* **1990**, *137*, 1657–1658. [[CrossRef](#)]
140. Tran, H.K.; Wu, Y.-S.; Chien, W.-C.; Wu, S.-H.; Jose, R.; Lue, S.J.; Yang, C.-C. Composite polymer electrolytes based on PVA/PAN for all-solid-state lithium metal batteries operated at room temperature. *ACS Appl. Energy Mater.* **2020**, *3*, 11024–11035. [[CrossRef](#)]
141. Chen, W.P.; Duan, H.; Shi, J.-L.; Qian, Y.; Wan, J.; Zhang, X.-D.; Sheng, H.; Guan, B.; Wen, R.; Yin, Y.-X.; et al. Bridging Interparticle Li<sup>+</sup> Conduction in a Soft Ceramic Oxide Electrolyte. *J. Am. Chem. Soc.* **2021**, *143*, 5717–5726. [[CrossRef](#)]
142. Wright, P.V. Electrical conductivity in ionic complexes of poly(ethylene oxide). *Br. Polym. J.* **1975**, *7*, 319–327. [[CrossRef](#)]
143. Yang, C.C.; Lin, S.J. Alkaline composite PEO-PVA-glass-fibre-mat polymer electrolyte for Zn-air battery. *J. Power Sources* **2002**, *112*, 497–503. [[CrossRef](#)]
144. Wen, Z.; Itoh, T.; Uno, T.; Kubo, M.; Yamamoto, O. Thermal, electrical, and mechanical properties of composite polymer electrolytes based on cross-linked poly(ethylene oxide-co-propylene oxide) and ceramic filler. *Solid State Ion.* **2003**, *160*, 141–148. [[CrossRef](#)]
145. Xu, S.; Sun, Z.; Sun, C.; Li, F.; Chen, K.; Zhang, Z.; Hou, G.; Cheng, H.; Li, F. Homogeneous and Fast Ion Conduction of PEO-Based Solid-State Electrolyte at Low Temperature. *Adv. Funct. Mater.* **2020**, *30*, 2007172. [[CrossRef](#)]
146. Fauteux, D.; Massucco, A.; McLin, M.; Van Buren, M.; Shi, J. Lithium polymer electrolyte rechargeable battery. *Electrochim. Acta* **1995**, *40*, 2185–2190. [[CrossRef](#)]
147. Weston, J.; Steele, B. Effects of inert fillers on the mechanical and electrochemical properties of lithium salt-poly(ethylene oxide) polymer electrolytes. *Solid State Ion.* **1982**, *7*, 75–79. [[CrossRef](#)]
148. Zhang, D.; Li, L.; Wu, X.; Wang, J.; Li, Q.; Pan, K.; He, J. Research Progress and Application of PEO-Based Solid State Polymer Composite Electrolytes. *Front. Energy Res.* **2021**, *9*, 726738. [[CrossRef](#)]
149. Li, C.; Xue, P.; Chen, L.; Liu, J.; Wang, Z. Reducing the crystallinity of PEO-based composite electrolyte for high performance lithium batteries. *Compos. Part B Eng.* **2022**, *234*, 109729. [[CrossRef](#)]
150. He, K.; Cheng, S.H.; Hu, J.; Zhang, Y.; Yang, H.; Liu, Y.; Liao, W.; Chen, D.; Liao, C.; Cheng, X.; et al. In-Situ Intermolecular Interaction in Composite Polymer Electrolyte for Ultralong Life Quasi-Solid-State Lithium Metal Batteries. *Angew. Chem. Int. Ed.* **2021**, *60*, 12116–12123. [[CrossRef](#)]

151. Ramesh, S.; Wen, L.C. Investigation on the effects of addition of  $\text{SiO}_2$  nanoparticles on ionic conductivity, FTIR, and thermal properties of nanocomposite PMMA– $\text{LiCF}_3\text{SO}_3$ – $\text{SiO}_2$ . *Ionics* **2009**, *16*, 255–262. [CrossRef]
152. Jiang, Y.; Yan, X.; Ma, Z.; Mei, P.; Xiao, W.; You, Q.; Zhang, Y. Development of the PEO based solid polymer electrolytes for all-solid state lithium ion batteries. *Polymers* **2018**, *10*, 1237. [CrossRef]
153. Li, Y.J.; Fan, C.Y.; Zhang, J.P.; Wu, X.L. A promising PMHS/PEO blend polymer electrolyte for all-solid-state lithium ion batteries. *Dalton Trans.* **2018**, *47*, 14932–14937. [CrossRef]
154. Wang, G.; Zhu, X.; Rashid, A.; Hu, Z.; Sun, P.; Zhang, Q.; Zhang, L. Organic polymeric filler-amorphized poly(ethylene oxide) electrolyte enables all-solid-state lithium–metal batteries operating at 35 °C. *J. Mater. Chem. A* **2020**, *8*, 13351–13363. [CrossRef]
155. Amanchukwu, C.V.; Harding, J.R.; Shao-Horn, Y.; Hammond, P.T. Understanding the chemical stability of polymers for lithium-air batteries. *Chem. Mater.* **2015**, *27*, 550–561. [CrossRef]
156. Uludağ, A.A.; Tokur, M.; Algul, H.; Cetinkaya, T.; Uysal, M.; Akbulut, H. High stable Li-air battery cells by using PEO and PVDF additives in the TEGDME/LiPF<sub>6</sub> electrolytes. *Int. J. Hydrogen Energy* **2016**, *41*, 6954–6964. [CrossRef]
157. Stephan, A.M. Review on gel polymer electrolytes for lithium batteries. *Eur. Polym. J.* **2006**, *42*, 21–42. [CrossRef]
158. Gopalan, A.I.; Santhosh, P.; Manesh, K.M.; Nho, J.H.; Kim, S.H.; Hwang, C.-G.; Lee, K.-P. Development of electrospun PVdF-PAN membrane-based polymer electrolytes for lithium batteries. *J. Membr. Sci.* **2008**, *325*, 683–690. [CrossRef]
159. Ramesh, S.; Lu, S.-C. Enhancement of ionic conductivity and structural properties by 1-butyl-3-methylimidazolium trifluoromethanesulfonate ionic liquid in poly(vinylidene fluoride-hexafluoropropylene)-based polymer electrolytes. *J. Appl. Polym. Sci.* **2012**, *126*, E484–E492. [CrossRef]
160. Kim, K.M.; Ryu, K.S.; Kang, S.-G.; Chang, S.H.; Chung, I.J. The Effect of Silica Addition on the Properties of Poly((vinylidene fluoride)-co-hexafluoropropylene)-Based Polymer Electrolytes. *Macromol. Chem. Phys.* **2001**, *202*, 866–872. [CrossRef]
161. Saikia, D.; Chen-Yang, Y.; Chen, Y.; Li, Y.; Lin, S. Investigation of ionic conductivity of composite gel polymer electrolyte membranes based on P(VDF-HFP), LiClO<sub>4</sub> and silica aerogel for lithium ion battery. *Desalination* **2008**, *234*, 24–32. [CrossRef]
162. Liu, T.; Chang, Z.; Yin, Y.; Chen, K.; Zhang, Y.; Zhang, X. The PVDF-HFP gel polymer electrolyte for Li-O<sub>2</sub> battery. *Solid State Ion.* **2018**, *318*, 88–94. [CrossRef]
163. Wang, Y.; Huang, K.; Zhang, P.; Li, H.; Mi, H. PVDF-HFP based polymer electrolytes with high Li<sup>+</sup> transference number enhancing the cycling performance and rate capability of lithium metal batteries. *Appl. Surf. Sci.* **2021**, *574*, 151593. [CrossRef]
164. Celik, M.; Kizilaslan, A.; Can, M.; Cetinkaya, T.; Akbulut, H. Electrochemical investigation of PVDF: HFP gel polymer electrolytes for quasi-solid-state Li-O<sub>2</sub> batteries: Effect of lithium salt type and concentration. *Electrochim. Acta* **2021**, *371*, 137824. [CrossRef]
165. Rajendran, S.; Mahendran, O.; Kannan, R. Ionic conductivity studies in composite solid polymer electrolytes based on methyl-methacrylate. *J. Phys. Chem. Solids* **2002**, *63*, 303–307. [CrossRef]
166. Liew, C.; Durairaj, R.; Ramesh, S. Rheological studies of PMMA-PVC based polymer blend electrolytes with LiTFSI as doping salt. *PLoS ONE* **2014**, *9*, e102815. [CrossRef] [PubMed]
167. Jahn, M.; Sedlářková, M.; Vondrák, J.; Pařízek, L. PMMA-Based Electrolytes for Li-Ion Batteries. *ECS Trans.* **2016**, *74*, 159–164. [CrossRef]
168. Flora, X.H.; Ulaganathan, M.; Babu, R.S.; Rajendran, S. Evaluation of lithium ion conduction in PAN/PMMA-based polymer blend electrolytes for Li-ion battery applications. *Ionics* **2012**, *18*, 731–736. [CrossRef]
169. Wang, S.; Hu, J.; Gui, X.; Lin, S.; Tu, Y. A Promising PMMA/m-MgO All-Solid-State Electrolyte for Lithium-Oxygen Batteries. *J. Electrochem. Soc.* **2021**, *168*, 020514. [CrossRef]
170. Liu, X.; Xin, X.; Shen, L.; Gu, Z.; Wu, J.; Yao, X. Poly(methyl methacrylate)-Based Gel Polymer Electrolyte for High-Performance Solid State Li-O<sub>2</sub> Battery with Enhanced Cycling Stability. *ACS Appl. Energy Mater.* **2021**, *4*, 3975–3982. [CrossRef]
171. Kim, Y.D.; Jo, Y.K.; Jo, N.J. Electrochemical performance of poly(vinyl alcohol)-based solid polymer electrolyte for lithium polymer batteries. *J. Nanosci. Nanotechnol.* **2012**, *12*, 3529–3533. [CrossRef]
172. Yang, C.C.; Wu, G. Study of microporous PVA/PVC composite polymer membrane and its application to MnO<sub>2</sub> capacitors. *Mater. Chem. Phys.* **2009**, *114*, 948–955. [CrossRef]
173. Rajendran, S.; Sivakumar, M.; Subadevi, R. Effect of salt concentration in poly(vinyl alcohol)-based solid polymer electrolytes. *J. Power Sources* **2003**, *124*, 225–230. [CrossRef]
174. Yang, J.M.; Wang, H.Z.; Yang, C.C. Modification and characterization of semi-crystalline poly(vinyl alcohol) with interpenetrating poly(acrylic acid) by UV radiation method for alkaline solid polymer electrolytes membrane. *J. Membr. Sci.* **2008**, *322*, 74–80. [CrossRef]
175. He, Y.; Li, S.; Zhou, S.; Hu, H. Mechanical integrity degradation and control of all-solid-state lithium battery with physical aging poly (vinyl alcohol)-based electrolyte. *Polymers* **2020**, *12*, 1886. [CrossRef] [PubMed]
176. Wang, C.; Liang, J.; Zhao, Y.; Zheng, M.; Li, X.; Sun, X. All-solid-state lithium batteries enabled by sulfide electrolytes: From fundamental research to practical engineering design. *Energy Environ. Sci.* **2021**, *14*, 2577–2619. [CrossRef]
177. Song, S.; Qin, X.; Ruan, Y.; Li, W.; Xu, Y.; Zhang, D.; Thokchom, J. Enhanced performance of solid-state lithium-air batteries with continuous 3D garnet network added composite polymer electrolyte. *J. Power Sources* **2020**, *461*, 228146. [CrossRef]
178. Castillo, J.; Santiago, A.; Judez, X.; Garbayo, I.; Clemente, J.A.C.; Morant-Miñana, M.C.; Villaverde, A.; González-Marcos, J.A.; Zhang, H.; Armand, M.; et al. Safe, Flexible, and High-Performing Gel-Polymer Electrolyte for Rechargeable Lithium Metal Batteries. *Chem. Mater.* **2021**, *33*, 8812–8821. [CrossRef]

179. Dirican, M.; Yan, C.; Zhu, P.; Zhang, X. Composite solid electrolytes for all-solid-state lithium batteries. *Mater. Sci. Eng. R Rep.* **2018**, *136*, 27–46. [[CrossRef](#)]
180. Wang, J.; Huang, G.; Yan, J.-M.; Ma, J.-L.; Liu, T.; Shi, M.-M.; Yu, Y.; Zhang, M.-M.; Tang, J.-L.; Zhang, X.-B. Hybrid solid electrolyte enabled dendrite-free Li anodes for high-performance quasi-solid-state lithium-oxygen batteries. *Natl. Sci. Rev.* **2020**, *8*, nwaa150. [[CrossRef](#)]
181. Ouyang, H.; Min, S.; Yi, J.; Liu, X.; Ning, F.; Qin, J.; Jiang, Y.; Zhao, B.; Zhang, J. Tuning composite solid-state electrolyte interface to improve the electrochemical performance of lithium-oxygen battery. *Green Energy Environ.* **2022**, *8*, 1195–1204. [[CrossRef](#)]
182. Wang, S.; Wang, J.; Liu, J.; Song, H.; Liu, Y.; Wang, P.; He, P.; Xu, J.; Zhou, H. Ultra-fine surface solid-state electrolytes for long cycle life all-solid-state lithium-air batteries. *J. Mater. Chem. A* **2018**, *6*, 21248–21254. [[CrossRef](#)]
183. Wu, B.; Wang, S.; Iv, W.J.E.; Deng, D.Z.; Yang, J.; Xiao, J. Interfacial behaviours between lithium ion conductors and electrode materials in various battery systems. *J. Mater. Chem. A* **2016**, *4*, 15266–15280. [[CrossRef](#)]
184. Zhao, C.; Liang, J.; Li, X.; Holmes, N.; Wang, C.; Wang, J.; Zhao, F.; Li, S.; Sun, Q.; Yang, X.; et al. Halide-based solid-state electrolyte as an interfacial modifier for high performance solid-state Li-O<sub>2</sub> batteries. *Nano Energy* **2020**, *75*, 105036. [[CrossRef](#)]
185. Zhao, C.; Sun, Q.; Luo, J.; Liang, J.; Liu, Y.; Zhang, L.; Wang, J.; Deng, S.; Lin, X.; Yang, X.; et al. 3D Porous Garnet/Gel Polymer Hybrid Electrolyte for Safe Solid-State Li-O<sub>2</sub> Batteries with Long Lifetimes. *Chem. Mater.* **2020**, *32*, 10113–10119. [[CrossRef](#)]
186. Chamaani, A.; Chawla, N.; Safa, M.; El-Zahab, B. One-Dimensional Glass Micro-Fillers in Gel Polymer Electrolytes for Li-O<sub>2</sub> Battery Applications. *Electrochim. Acta* **2017**, *235*, 56–63. [[CrossRef](#)]
187. Luo, K.; Zhu, G.; Zhao, Y.; Luo, Z.; Liu, X.; Zhang, K.; Li, Y.; Scott, K. Enhanced cycling stability of Li-O<sub>2</sub> batteries by using a polyurethane/SiO<sub>2</sub>/glass fiber nanocomposite separator. *J. Mater. Chem. A* **2018**, *6*, 7770–7776. [[CrossRef](#)]
188. Ma, C.; Zhang, J.; Xu, M.; Xia, Q.; Liu, J.; Zhao, S.; Chen, L.; Pan, A.; Ivey, D.G.; Wei, W. Cross-linked branching nanohybrid polymer electrolyte with monodispersed TiO<sub>2</sub> nanoparticles for high performance lithium-ion batteries. *J. Power Sources* **2016**, *317*, 103–111. [[CrossRef](#)]
189. Zhu, X.B.; Zhao, T.S.; Wei, Z.H.; Tan, P.; Zhao, G. A novel solid-state Li-O<sub>2</sub> battery with an integrated electrolyte and cathode structure. *Energy Environ. Sci.* **2015**, *8*, 2782–2790. [[CrossRef](#)]
190. Zhu, X.B.; Zhao, T.S.; Wei, Z.H.; Tan, P.; An, L. A high-rate and long cycle life solid-state lithium-air battery. *Energy Environ. Sci.* **2015**, *8*, 3745–3754. [[CrossRef](#)]
191. Zhu, X.; Zhao, T.; Tan, P.; Wei, Z.; Wu, M. A high-performance solid-state lithium-oxygen battery with a ceramic-carbon nanostructured electrode. *Nano Energy* **2016**, *26*, 565–576. [[CrossRef](#)]
192. Ren, Y.; Deng, H.; Zhao, H.; Zhou, Z.; Wei, Z. A simple and effective method to prepare dense Li<sub>1.3</sub>Al<sub>0.3</sub>Ti<sub>1.7</sub>(PO<sub>4</sub>)<sub>3</sub> solid-state electrolyte for lithium-oxygen batteries. *Ionics* **2020**, *26*, 6049–6056. [[CrossRef](#)]
193. Gong, H.; Xue, H.; Lu, X.; Gao, B.; Wang, T.; He, J.; Ma, R. All solid-state lithium-oxygen batteries with MOF-derived nickel cobaltate nanoflake arrays as high-performance oxygen cathodes. *Chem. Commun.* **2019**, *55*, 10689–10692. [[CrossRef](#)]
194. Zhao, C.; Zhu, Y.; Sun, Q.; Wang, C.; Luo, J.; Lin, X.; Yang, X.; Zhao, Y.; Li, R.; Zhao, S.; et al. Transition of the Reaction from Three-Phase to Two-Phase by Using a Hybrid Conductor for High-Energy-Density High-Rate Solid-State Li-O<sub>2</sub> Batteries. *Angew. Chem. Int. Ed.* **2021**, *60*, 5821–5826. [[CrossRef](#)]
195. Sun, J.; Zhao, N.; Li, Y.; Guo, X.; Feng, X.; Liu, X.; Liu, Z.; Cui, G.; Zheng, H.; Gu, L.; et al. A rechargeable Li-air fuel cell battery based on garnet solid electrolytes. *Sci. Rep.* **2017**, *7*, srep41217. [[CrossRef](#)]
196. Jiang, F.; Ma, L.; Sun, J.; Guo, L.; Peng, Z.; Cui, Z.; Li, Y.; Guo, X.; Zhang, T. Deciphering the Enigma of Li<sub>2</sub>CO<sub>3</sub> Oxidation Using a Solid-State Li-Air Battery Configuration. *ACS Appl. Mater. Interfaces* **2021**, *13*, 14321–14326. [[CrossRef](#)]
197. Wang, J.; Yin, Y.; Liu, T.; Yang, X.; Chang, Z.; Zhang, X. Hybrid electrolyte with robust garnet-ceramic electrolyte for lithium anode protection in lithium-oxygen batteries. *Nano Res.* **2018**, *11*, 3434–3441. [[CrossRef](#)]
198. Kufian, M.; Ramesh, S.; Arof, A. PMMA-LiTFSI based gel polymer electrolyte for lithium-oxygen cell application. *Opt. Mater.* **2021**, *120*, 111418. [[CrossRef](#)]
199. Xu, Z.; Liu, Z.; Gu, Z.; Zhao, X.; Guo, D.; Yao, X. Polyimide-Based Solid-State Gel Polymer Electrolyte for Lithium-Oxygen Batteries with a Long-Cycling Life. *ACS Appl. Mater. Interfaces* **2023**, *15*, 7014–7022. [[CrossRef](#)]
200. Wang, J.; Huang, G.; Chen, K.; Zhang, X. An Adjustable-Porosity Plastic Crystal Electrolyte Enables High-Performance All-Solid-State Lithium-Oxygen Batteries. *Angew. Chem. Int. Ed.* **2020**, *59*, 9382–9387. [[CrossRef](#)]
201. Kumar, B.; Kumar, J. Cathodes for Solid-State Lithium–Oxygen Cells: Roles of Nasicon Glass-Ceramics. *J. Electrochem. Soc.* **2010**, *157*, A611–A616. [[CrossRef](#)]
202. Balaish, M.; Peled, E.; Golodnitsky, D.; Ein-Eli, Y. Liquid-Free Lithium-Oxygen Batteries. *Angew. Chem. Int. Ed.* **2014**, *54*, 436–440. [[CrossRef](#)]
203. Yu, W.; Xue, C.; Hu, B.; Xu, B.; Li, L.; Nan, C.-W. Oxygen- and dendrite-resistant ultra-dry polymer electrolytes for solid-state Li-O<sub>2</sub> batteries. *Energy Storage Mater.* **2020**, *27*, 244–251. [[CrossRef](#)]
204. Yi, J.; Liu, Y.; Qiao, Y.; He, P.; Zhou, H. Boosting the Cycle Life of Li-O<sub>2</sub> Batteries at Elevated Temperature by Employing a Hybrid Polymer-Ceramic Solid Electrolyte. *ACS Energy Lett.* **2017**, *2*, 1378–1384. [[CrossRef](#)]
205. Yang, T.; Shu, C.; Zheng, R.; Hu, A.; Hou, Z.; Li, M.; Ran, Z.; Hei, P.; Long, J. Excellent electrolyte-electrode interface stability enabled by inhibition of anion mobility in hybrid gel polymer electrolyte based Li-O<sub>2</sub> batteries. *J. Membr. Sci.* **2020**, *604*, 118051. [[CrossRef](#)]

206. Wu, S.; Yi, J.; Zhu, K.; Bai, S.; Liu, Y.; Qiao, Y.; Ishida, M.; Zhou, H. A Super-Hydrophobic Quasi-Solid Electrolyte for Li-O<sub>2</sub> Battery with Improved Safety and Cycle Life in Humid Atmosphere. *Adv. Energy Mater.* **2016**, *7*, 1601759. [CrossRef]
207. Shu, C.; Long, J.; Dou, S.; Wang, J. Component-Interaction Reinforced Quasi-Solid Electrolyte with Multifunctionality for Flexible Li-O<sub>2</sub> Battery with Superior Safety under Extreme Conditions. *Small* **2019**, *15*, e1804701. [CrossRef]
208. Chawla, N.; Chamaani, A.; Safa, M.; Herndon, M.; El-Zahab, B. Mechanism of ionic impedance growth for palladium-containing cnt electrodes in lithium-oxygen battery electrodes and its contribution to battery failure. *Batteries* **2019**, *5*, 15. [CrossRef]
209. Kim, M.; Lee, H.; Kwon, H.J.; Bak, S.-M.; Jaye, C.; Fischer, D.A.; Yoon, G.; Park, J.O.; Seo, D.-H.; Ma, S.B.; et al. Carbon-free high-performance cathode for solid-state Li-O<sub>2</sub> battery. *Sci. Adv.* **2022**, *8*, abm8584. [CrossRef]
210. Pakseresht, S.; Al-Ogaili, A.W.M.; Cetinkaya, T.; Celik, M.; Akbulut, H. Prevention of side reactions with a unique carbon-free catalyst biosynthesized by a virus template for non-aqueous and quasi-solid-state Li-O<sub>2</sub> batteries. *J. Power Sources* **2021**, *509*, 230374. [CrossRef]
211. Li, C.; Liu, Y.; Li, B.; Zhang, F.; Cheng, Z.; He, P.; Zhou, H. Integrated solid electrolyte with porous cathode by facilely one-step sintering for an all-solid-state Li-O<sub>2</sub> battery. *Nanotechnology* **2019**, *30*, 364003. [CrossRef]
212. Li, C.; Huang, G.; Yu, Y.; Xiong, Q.; Yan, J.; Zhang, X. Three Birds with One Stone: An Integrated Cathode–Electrolyte Structure for High-Performance Solid-State Lithium–Oxygen Batteries. *Small* **2022**, *18*, 2107833. [CrossRef] [PubMed]
213. Muthukumaran, A.; Ravichandran, A.; Shanbhag, S.; Arjun, R.; Rengaswamy, R. Lithium-air battery electrocatalyst identification using Machine Learning and SciBERT word embeddings. In *Computer Aided Chemical Engineering*; Elsevier: Amsterdam, The Netherlands, 2022; Volume 51, pp. 1429–1434. [CrossRef]
214. Sharma, P.; Bora, B.J. A Review of Modern Machine Learning Techniques in the Prediction of Remaining Useful Life of Lithium-Ion Batteries. *Batteries* **2022**, *9*, 13. [CrossRef]
215. Wang, A.; Zou, Z.; Wang, D.; Liu, Y.; Li, Y.; Wu, J.; Avdeev, M.; Shi, S. Identifying Chemical Factors Affecting Reaction Kinetics in Li-air Battery via ab initio Calculations and Machine Learning. *Energy Storage Mater.* **2020**, *35*, 595–601. [CrossRef]
216. Mishra, A.K.; Rajput, S.; Karamta, M.; Mukhopadhyay, I. Exploring the Possibility of Machine Learning for Predicting Ionic Conductivity of Solid-State Electrolytes. *ACS Omega* **2023**, *8*, 16419–16427. [CrossRef]
217. Waidha, A.I.; Salihovic, A.; Jacob, M.; Vanita, V.; Aktekin, B.; Brix, K.; Wissel, K.; Kautenburger, R.; Janek, J.; Ensinger, W.; et al. Recycling of All-Solid-State Li-ion Batteries: A Case Study of the Separation of Individual Components Within a System Composed of LTO, LLZTO and NMC. *Chemsuschem* **2023**, *16*, e202202361. [CrossRef] [PubMed]
218. Barbosa, J.C.; Gonçalves, R.; Costa, C.M.; Lanceros-Méndez, S. Toward Sustainable Solid Polymer Electrolytes for Lithium-Ion Batteries. *ACS Omega* **2022**, *7*, 14457–14464. [CrossRef] [PubMed]
219. Schwich, L.; Küpers, M.; Finsterbusch, M.; Schreiber, A.; Fattakhova-Rohlfing, D.; Guillon, O.; Friedrich, B. Recycling strategies for ceramic all-solid-state batteries—Part i: Study on possible treatments in contrast to li-ion battery recycling. *Metals* **2020**, *10*, 1523. [CrossRef]
220. Bubulinca, C.; Kazantseva, N.E.; Pechancova, V.; Joseph, N.; Fei, H.; Venher, M.; Ivanichenko, A.; Saha, P. Development of All-Solid-State Li-Ion Batteries: From Key Technical Areas to Commercial Use. *Batteries* **2023**, *9*, 157. [CrossRef]

**Disclaimer/Publisher's Note:** The statements, opinions and data contained in all publications are solely those of the individual author(s) and contributor(s) and not of MDPI and/or the editor(s). MDPI and/or the editor(s) disclaim responsibility for any injury to people or property resulting from any ideas, methods, instructions or products referred to in the content.